Seismic stratigraphic framework and structural evolution of the eastern Scotian Slope: geological context for the NS14-1 Call for Bids area, offshore Nova Scotia

Mark E. Deptuck, Kris Kendell, David E. Brown, Brenton M. Smith

Canada-Nova Scotia Offshore Petroleum Board, Halifax, Nova Scotia, Canada

Introduction and scope

This report summarizes the Mesozoic to Cenozoic geology of the eastern Scotian Slope, between The Gully (a large submarine canyon that bisects the shelf and slope just east of Sable Island), and the Laurentian Channel (a 100 km wide shelf-crossing trough that formed during Quaternary advance and retreat of glacial ice; Piper et al., 2012) (Fig. 1). Results are based primarily on reflection seismic profiles tied to industry wells. The primary objective is to provide geological context for Parcels 1 through 4 in the CNSOPB NS14-1 Call for Bids. The Call area is best known geologically for a unique structural element known as the "Banquereau Synkinematic Wedge" (**BSW**; Shimeld, 2004). The BSW is a large Middle to Late Jurassic (Ings and Shimeld, 2006) or earliest Cretaceous (OETR, 2011) salt-based detachment overlain by a range of potential hydrocarbon-bearing structures that include roho systems, inverted minibasins, and rim synclines that were variably transported down the slope and compressed during at least two periods of shortening. The Call area also crosses an important geological boundary, where the BSW and the allochthonous salt along its base are juxtaposed with a primary (autochthonous) salt basin to the northeast (the southwestern Laurentian Subbasin; **SWLS**)(Fig. 2). Although much of the salt in the BSW was supplied from a primary salt basin to the northwest (the Huron Subbasin; CNSOPB, 2013), the salt-based detachment in the eastern part of the BSW appears to have developed above salt that was expelled from the SWLS. Salt-related structures in the SWLS are complex, with stepped counter-regional systems and seaward leaning feeders expelling salt into a large salt-stock or salt-tongue canopy that was subsequently re-loaded and variably squeezed. As many as three tiers of allochthonous salt are present here, creating a wide variety of potential trap configurations, but also substantially degrading seismic imaging across much of the SWLS.

We provide a detailed account of the stratigraphic and structural evolution of the eastern Scotian Slope before, during, and after development of the BSW, and the co-evolution of the SWLS to its east. We also attempt to link the broad-scale structural and seismic stratigraphic changes in the NS14-1 Call area on the slope to the development of shelf depositional systems that have been calibrated with wells landward of the Call area (and described in CNSOPB, 2013). Particular focus is placed on the distribution, timing and style of potential hydrocarbon-bearing structures and potential reservoir intervals on the slope.

Study area and parcel location

The primary study area for this report includes the outermost Scotian Shelf, Scotian Slope, and proximal Sohm Abyssal Plain (Figs. 1, 2). NS14-1 Parcels 1 to 4 are located in the southern half of the study area, principally on the modern continental slope. Parcels 1 and 2 are located on the upper to lower slope in the western Call area, in water depths ranging from about 150 to 4100 m. They cover the proximal to distal reaches of the BSW. Parcel 3 is located on the upper to middle slope and covers the SWLS, in water depths ranging from about 100 to 3100 m. Parcel 4 is located on the middle to lower slope in water depths ranging from 2200 to 4100 m. It covers a complex region of suturing and salt expulsion from both the BSW and the SWLS. Both Parcels 3 and 4 border the Nova Scotia –
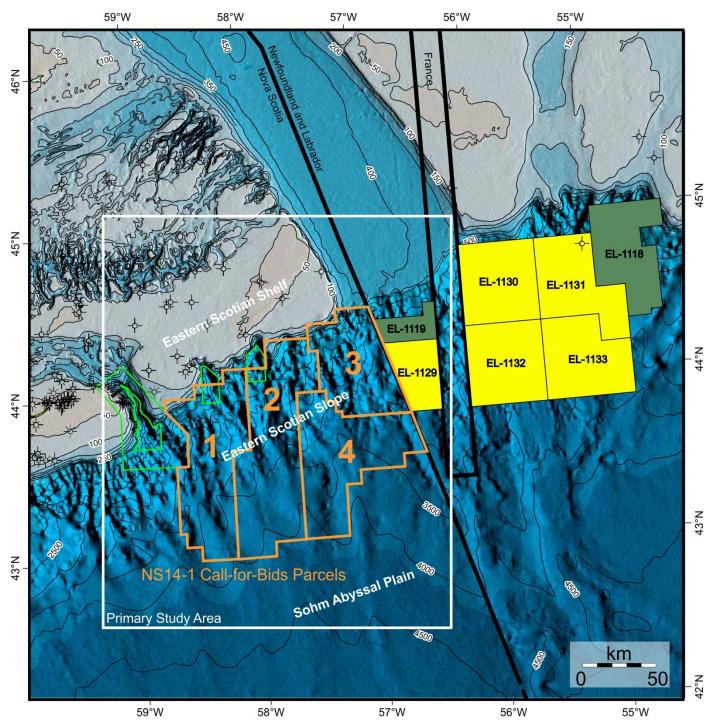
Figure 1. Regional bathymetric map showing the primary study area and the location of NS14-1 Call for Bids parcels 1 to 4. Also shown are active C-NLOPB exploration licenses. Bathymetry fro NOAA ETOPO1.

Newfoundland and Labrador jurisdictional boundary, adjacent to active C-NLOPB exploration licenses (Fig. 1).

Geological setting and previous work

The present-day configuration of the Scotian margin began to take shape in the early Mesozoic during rifting of Pangea, between what is now Nova Scotia and Morocco in the central North Atlantic. At the onset of rifting (Middle Triassic), the Scotian margin was underlain by basement comprised of lower Paleozoic metasedimentary rocks of the Meguma Supergroup that were later intruded by mid-Paleozoic plutonic rocks (Pe-Piper and Jansa, 1999), and overlain locally by Carboniferous sedimentary basins (e.g. Pascucci et al., 1999; Waldron et al., 2010). An important Mesozoic strike-slip fault zone, referred to as the 'southwest Grand Banks transform margin' (Pe-Piper and Piper, 2004), cuts through the northern parts of Figures 2 and 3 (trending parallel to the "Collector Anomaly" in this area). It forms a westward continuation of the northwest trending Newfoundland Fracture Zone, and closely coincides with an important Mesozoic hinge zone where basement depth increases abruptly to the south. The trace of the hinge zone continues to the west where it forms the northern boundary of the Orpheus Graben, and continues onshore and into the Fundy Basin as the Cobequid-Chedabucto fault system (Wade and MacLean, 1990; MacLean and Wade, 1992; Jansa et al., 1993; Pe-Piper and Piper, 2004; Pe-Piper et al., 2007). On magnetic maps, this strike-slip zone closely follows the trend of the "Collector Anomaly" that separates rocks of the Avalon terrane to the north from rocks of the Meguma terrane to the south (Haworth and Lefort, 1979; Fig. 3). As such, the SW Grand Banks transform margin probably formed, in part, along a reactivated Paleozoic lineament (Keen et al., 1990), and was intermittently active through the Mesozoic and perhaps into the Tertiary (Pe-Piper and Piper, 2004). Early and mid-Cretaceous volcanism on the southern Grand Banks and near the Orpheus Graben, respectively, record periods of reactivation along parts of this terrane boundary (Wade and MacLean, 1990; Pe-Piper and Piper, 2004; Pe-Piper et al., 2007).

On the Scotian Shelf south of the transform margin, Triassic crustal extension produced a series of east-west to northeast-southwest trending grabens and half grabens (Wade and MacLean, 1990; CNSOPB, 2013). Non-marine fluvial-lacustrine-playa synrift sediments accumulated in these narrow rift-basins, giving way both laterally (towards the rift axis) and up-section to widespread accumulations of salt during intermittent latest Triassic marine incursions (Wade and MacLean, 1990) (Fig. 4). Rifting on the Scotian margin lasted between 20 and 30 m.y. (Keen and Beaumont, 1990), with salt believed to have accumulated during rifting or near the end of rifting, potentially into the earliest postrift (Deptuck, 2011). Salt was thickest along the axes of these rift basins, thinning above or terminating along intervening basement highs like the Canso, Missisauga, and South Griffin ridges (Kendell, 2012; CNSOPB, 2013; Fig. 2). A second important hinge zone developed along the southern boundary of the Canso Ridge, with basement depth increasing to the south. The Huron Subbasin located seaward of this hinge zone and immediately landward of the South Griffin Ridge (OETR, 2011; CNSOPB, 2013), was a primary repository for Upper Triassic to Lower Jurassic salt (Argo Formation). Much of this salt was expelled onto the slope in response to Middle to Late Jurassic sediment loading coupled with an increase in margin tilt in response to thermal subsidence (Shimeld, 2004; Ings and Shimeld, 2006; Albertz et al. 2010).

The origin of basement rocks found seaward of the South Griffin Ridge is disputed. On the eastern Scotian Slope there is a weaker continuation of the East Coast Magnetic Anomaly (ECMA; Fig. 3), widely interpreted to mark the continent-ocean boundary further south (e.g. Klitgord and Schouten, 1986; Keen et al., 1990; Dehler, 2010; Labails et al., 2010). On the southwestern Scotian Slope this anomaly has been linked to the development of a volcanic margin with seaward dipping reflections (SDRs) found along the seaward edge of an
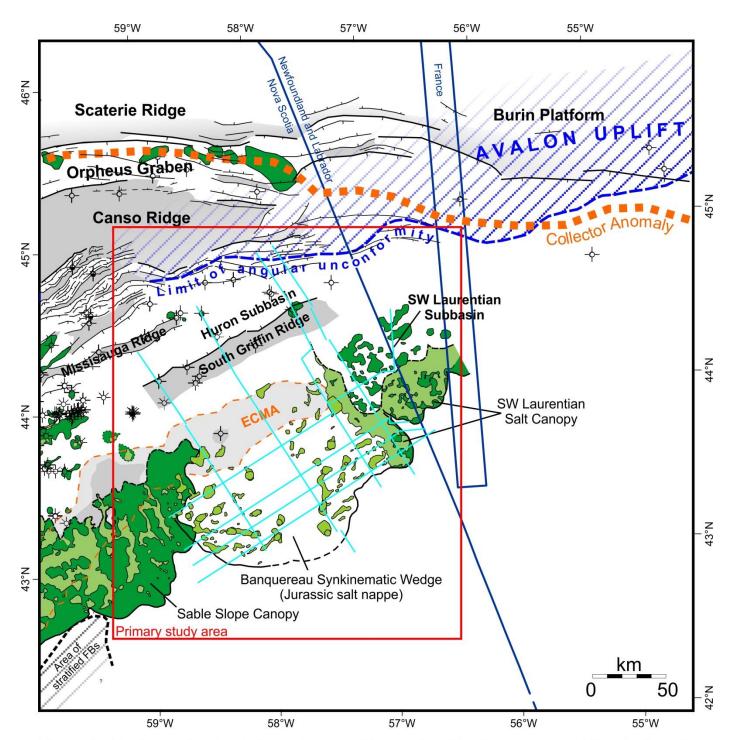
Figure 2. Regional structural elements map of the eastern Scotian margin and the shelf south of Newfoundland. The trend of the Avalon Uplift is shown in the blue hachured area, with the limit of the related angular unconformity (limit of Jurassic erosion) shown by the blue dashed line. Salt shown in green, with intervals of thicker canopy salt shown in lighter green. Basement highs are shaded grey. Location of magnetic anomalies shown in orange dashed lines. Regional dip and strike seismic sections shown in light blue. Some faults, and the salt in the Orpheus Graben are adapted from Wade and MacLean (1990) and MacLean and Wade (1992). Salt in the Sable Subbasin is from Kendell (2012). Primary study area shown in the red box.
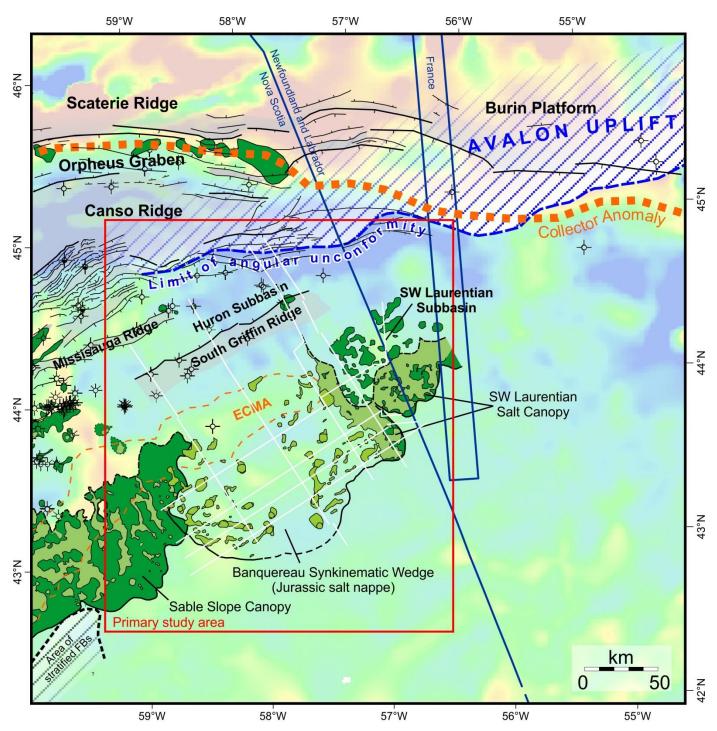
Figure 3. Regional structural elements map of the eastern Scotian margin and the shelf south of Newfoundland, overlain on a magnetics map (from Oakey and Dehler, 2004). See figure 2 caption for details about map elements.

autochthonous salt basin (Keen and Potter, 1995; Wu et al., 2006; Dehler, 2010, 2012; Deptuck, 2011; OETR, 2011). The weaker and more discontinuous eastern extension of the ECMA, however, has been variously interpreted as *(a)* a buried volcanic ridge (extending the volcanic margin all the way to the SW Newfoundland transform margin; e.g. OETR, 2011); *(b)* exhumed mantle emplaced after a rift jump (formed during mantle exposure and serpentinization; e.g., Sibuet et al, 2012), *(c)* thinned continental crust underlain by partially serpentinized mantle (e.g. Funck et al., 2004; Wu et al., 2006; Louden et al., 2012) or *(d)* extended continental crust overlain by thin volcanic layers emplaced during break-up (e.g. Dehler, 2012). The rugose basement immediately to the southeast of the ECMA along the eastern parts of the margin (described in more detail in a later section) has been variously interpreted as partially to heavily serpentinized mantle (Funck et al., 2004; Lau et al., 2010; Louden et al., 2012) or very thin slow spreading oceanic crust above partially serpentinized mantle (Louden et al., 2012), serpentinized mantle with minor volcanics on top (Sibuet et al., 2012), or oceanic crust (OETR, 2011).

Post-rift sedimentation

Areas of thick salt accumulation on the shelf profoundly influenced later sedimentation, with salt expulsion accommodating thick successions of postrift Jurassic strata seaward of the Canso Ridge (Kendell, 2012; CNSOPB, 2013). The general distribution of Jurassic strata is illustrated nicely in figure 5. Immature Early to Middle Jurassic continental clastic sediments of the Mohican Formation (Wade and MacLean, 1990) were the first to load the salt (Fig. 4). This was followed by a mixed Upper Jurassic succession of alternating shallow marine clastics and carbonates that prograded across the eastern Scotian Shelf towards the South Griffin Ridge (**SGR**), ultimately filling the Huron Subbasin (corresponding to the Mic Mac Formation; MacLean and Wade, 1992).

The "Banquereau Synkinematic Wedge" (**BSW**) – a widespread salt detachment system (Shimeld, 2004) –

developed on the continental slope seaward of the SGR (Fig. 2). It forms an anomalous ~130 km wide by ~150 km long and up to 4.5 km thick wedge of slope strata displaying landward-dipping, sigmoid-shaped reflectors that sole out into a regional salt detachment (Ings and Shimeld, 2006; Albertz et al., 2010; this study). Two different interpretations have been proposed for its timing. Ings and Shimeld (2006) followed by Albertz et al. (2010) interpret the BSW as a primarily Middle to Upper Jurassic element that is time-equivalent to the Mic Mac Formation. In this scenario, the top Jurassic marker is correlated *above* the BSW, and the BSW largely pre-dates the latest Jurassic development of the Avalon Uplift (see below). In contrast, OETR (2011) interpret the BSW as a Berriasian feature that is largely time-equivalent to the lower parts of the Missisauga Formation. In this scenario, the near-top Jurassic marker (the J150 marker of OETR, 2011) is carried *below* the BSW, and the BSW is largely synchronous with the Avalon Uplift (and records a period of accelerated slope sedimentation in response to accelerated shelf erosion). We favour carrying our near-top Jurassic marker above the BSW, in agreement with Ings and Shimeld (2006) and Albertz et al. (2010) (as discussed in more detail in a later section).

Although final break-up with Morocco probably took place in the Early Jurassic (Jansa and Wade, 1975; Keen and Beaumont, 1990; Wade and MacLean, 1990; Labails et al., 2010; Sibuet et al., 2012), the eastern Scotian margin continued to experience the effects from younger rifting to the north. Rejuvenated rifting between the Grand Banks and Iberia in the latest Jurassic was accompanied by widespread uplift along a broad basement arch known as the "Avalon Uplift" (Jansa and Wade, 1975). This prominent basement element, which roughly parallels the SW Grand Banks transform margin, extended across the southern Grand Banks and onto the Burin Platform (Fig. 2). Widespread erosion of the Avalon Uplift led to the development of a prominent angular unconformity and penneplain surface (the "Avalon Unconformity" of Jansa and Wade, 1975) that is clearly recognized on reflection seismic
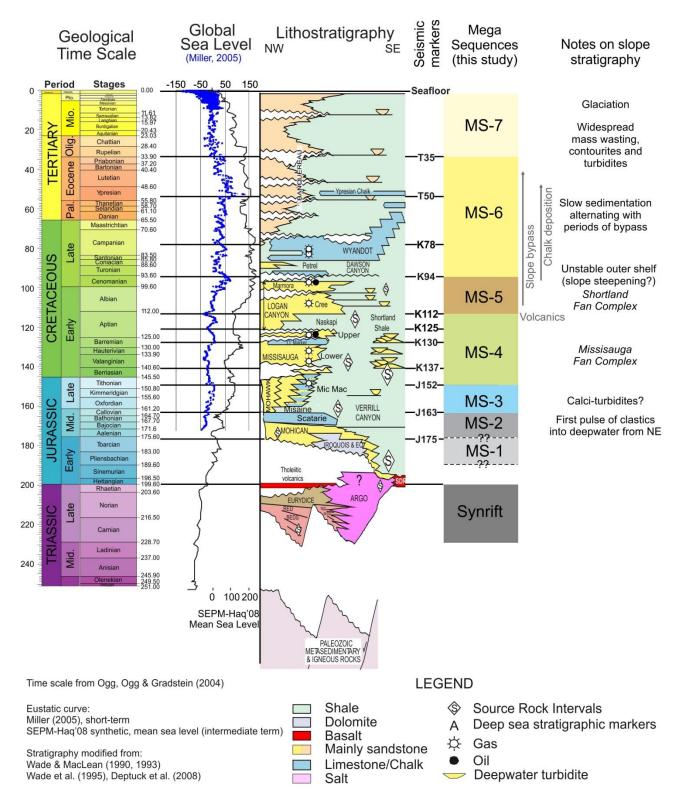
Figure 4. Stratigraphic column adpated from OETR (2011), with key seismic markers and mega-sequences 1 through 7 identified. Notes about slope stratigraphy are shown in the right hand column.
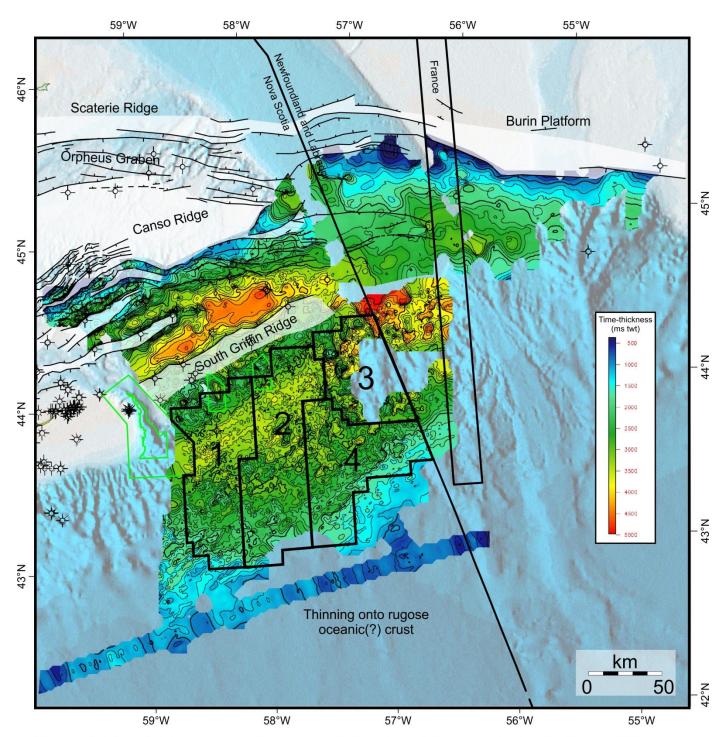
Figure 5. Time-thickness map of uppermost Triassic and Jurassic strata. On the shelf, the map is between the J152 marker and a marker correlated near the top of the synrift succession, but below the autochthonous salt layer. On the slope, the map is between the J152 marker and the top of the rugose basement. The succession corresponds closely to mega-sequences 1 to 3. See text for details.
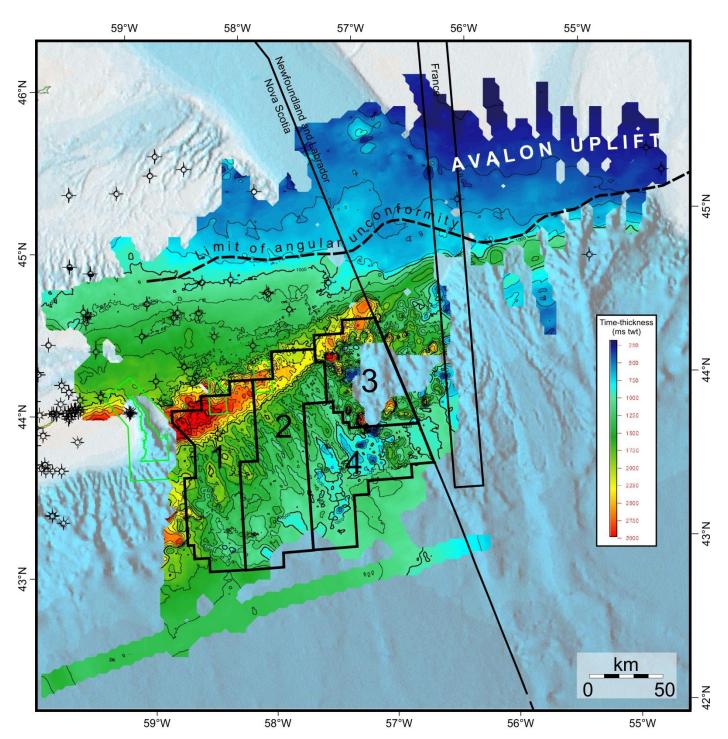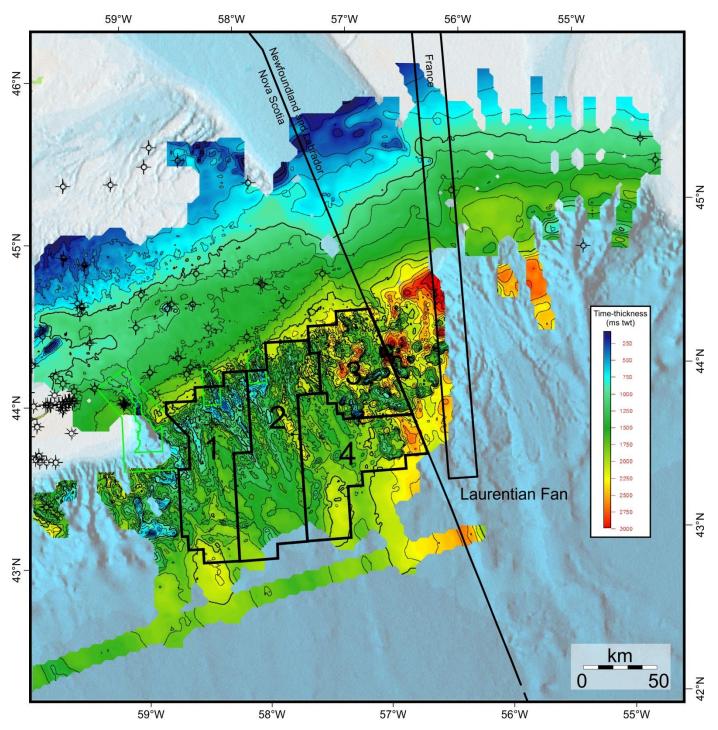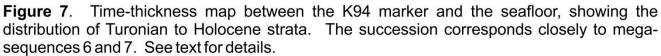
Figure 6. Time-thickness map between the J152 and K94 markers showing the prominent thinning of Cretaceous strata onto the angular unconformity associated with the latest Jurassic Avalon Uplift. The Missisauga and Logan Canyon formations, or their equivalents, onlap and drape the southwestern flank of the uplift, which had a profound influence on the broad-scale sediment distribution patterns in this important reservoir interval. The succession is closely equivalent to mega-sequences 4 and 5. See text for details.

Figure 7. Time-thickness map between the K94 marker and the seafloor, showing the distribution of Turonian to Holocene strata. The succession corresponds closely to mega-sequences 6 and 7. See text for details.

profiles. Jurassic and older strata were heavily eroded along this unconformity, especially north of 45° latitude (Fig. 2). Erosional truncation of Upper Jurassic strata has been traced as far west as the Canso Ridge (MacLean and Wade, 1992; this study). Likewise, the southwestern flank of the Avalon Uplift was onlapped by clastic-dominated Tithonian to Barremian fluvial-deltaic sediments of the Missisauga Formation during several transgressive-regressive cycles (Wade and MacLean, 1990). Aggradation and progradation of interbedded sandstone and shale units continued into the Cenomanian as the Logan Canyon Formation was deposited on a broad coastal plain and shallow shelf, with its more shale-prone basinal equivalent referred to informally as the "Shortland Shale" (Wade and MacLean, 1990). Pronounced thinning continued while the Logan Canyon Formation was deposited, and a combined thickness map of the Missisauga and Logan Canyon formations demonstrates the far-reaching and long-lived influence of the Avalon Uplift, even on the Scotian margin (Fig. 6).

In the Late Cretaceous through Eocene the margin was dominated by accumulations of pelagic chalks and marine shales that developed seaward of several shifting deltas that were largely perched on the shelf, landward of the continental shelf edge (Fensome et al., 2008; Smith et al., 2010; Weston et al., 2012; Deptuck and Campbell, 2012). The remaining post-Eocene succession is complex, with significant Miocene and Oligocene unconformities recorded on a shelf dominated by siliciclastics, and numerous mass transport deposits on the slope and abyssal plain that interfinger with contourites and turbidites (e.g. Campbell, 2011; Campbell and Deptuck, 2012; Piper et al., 2012) (Fig. 7).

Database and approach

Building on the seismic stratigraphic framework proposed in OETR (2011) and CNSOPB (2013), 12 regional seismic horizons were correlated across the shelf and slope of the study area (Fig. 4), and were used

to generate time-structure and time-thickness maps. For deeper horizons, on-the-fly post-stack filtering (band-pass Ormsby filter) was applied during horizon correlation to remove some of the frequency components (commonly below 4 Hz and varying amounts of the higher frequency component). The use of multiple filters allowed the highest confidence correlation of challenging markers like the top basement surface.

The seismic data-base is comprised of one 3D survey (referred to as the "Stonehouse 3D") and numerous 2D seismic programs that were collected during the 1980's to early 2000's (see Fig. 8 for a list of programs used). Middle Jurassic and younger strata on the outer shelf are calibrated by wells like W. Esperanto B-78, SW Banquereau F-34, Banquereau C-21, N. Banquereau I-13, Citadel H-52, Louisbourg J-47, S. Griffin J-13, Sachem D-76, Hesper P-52, and Dauntless D-35 (Fig. 9). Deepwater calibration is provided only by Tantallon M-41 for strata younger than Valanginian. Biostratigraphic interpretations from W. Esperanto B-78, Hesper P-52, Dauntless D-35, S. Griffin J-13, and Tantallon M-41 were recently re-examined by Weston et al. (2012) and their age designations are favoured in this report.

Because deepwater calibration in the study area is limited to Tantallon M-41 (Weston et al., 2012), age constraints for pre-Valanginian slope strata require correlation of shelf horizons across poorly imaged growth faults or must be based on other indirect lines of evidence like seismic stratigraphic relationships. Tentative age constraints for seismic markers outboard the BSW, on the Sohm Abyssal Plain, are however provided by Ebinger and Tucholke (1988) and Swift et al. (1986) who used sparse multichannel seismic profiles (collected in 1978) tied across long distances to Deep-Sea Drilling Project (DSDP) Site 384 on the J-Anomaly Ridge. For older seismic horizons (pre-Eocene), they also used the reflection terminations (pinch-outs) onto oceanic crust to propose maximum ages for seismic markers based on interpreted ages of magnetic anomalies. The Jurassic Magnetic Quiet Zone (JMQZ - Vogt, 1973), however, contains no coherent magnetic
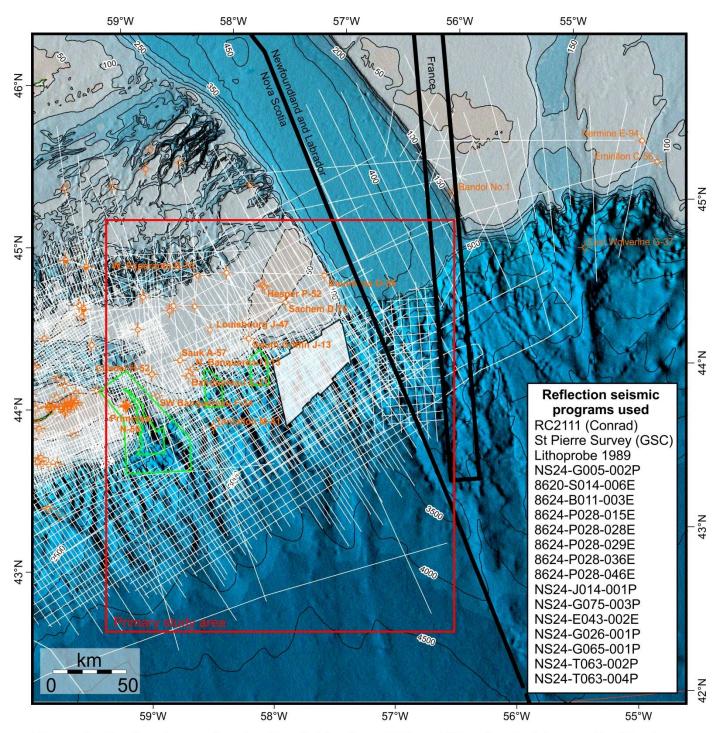
Figure 8. Regional map showing the distribution of 2D and 3D seismic data used in this study. Inset lists the program numbers/names. Key wells used in this study are bolded.

lineations outboard the ECMA, and so this approach for strata older than anomaly M22 (~151 Ma) required extrapolations of seafloor spreading half-rates from younger anomalies (Ebinger and Tucholke, 1988). Because there is some uncertainty regarding exactly where a given seismic marker pinches out, and additional uncertainty about Jurassic seafloor spreading rates, age constraints for pre-Mid-Jurassic strata in the Sohm Abyssal Plain in particular should be regarded as approximate.

Salt contact maps

Correlation of the intersection between the base salt surface (or its corresponding weld) and strata deposited in front of an advancing allochthonous salt body, provides a means of tracking the movement of salt through time, through the production of salt contact maps. In this study, preliminary salt contact maps were generated to better understand the relative timing and trajectory of salt expelled from the Huron and southwest Laurentian subbasins. Through time, the seaward boundary of the Banquereau salt nappe (described in a later section) and the corresponding salt-sediment contact, shift generally (but not exclusively) in the seaward direction. The ramp-to-flat geometry of the basal salt marker reflects a balance between the rate of horizontal salt advance and the rate of vertical sediment accumulation (Fletcher et al., 1995). During periods of rapid salt advance and/or slow sediment accumulation, the base salt surface will show only a very gradual low-angle climb up stratigraphic layers (producing a "flat") as it moves seaward. In such instances, there are larger error bars on the position of the salt contact because of increased uncertainty about where the seismic horizon terminates along the nearly parallel base salt surface. In contrast, during periods of slow horizontal salt advance and/or rapid sediment accumulation in front of the salt, the base salt surface will climb more abruptly through stratigraphic layers (producing a "ramp"). In such instances, the salt contacts are more confidently placed. In some instances, correlation of base salt ramps aided the generation of salt contact maps, and provided

additional constraints on the movement of allochthonous salt on the eastern Scotian Slope.

Line drawings and structure maps

Four composite dip sections were assembled from available seismic profiles, and line drawings were generated that serve as "down-slope" type sections across the eastern Scotian Slope (location shown in Fig. 9). From west to east they are named dip profiles D1, D2, D3 and D4 (Figs. 10, 11). Four composite strike sections were also assembled and line drawings from these serve as "cross-slope" type sections (from south to north named profiles S1, S2 (Fig. 12a) S3 and S4 (Fig. 12b). These type sections are used to track proximal to distal and lateral thickness variations between key seismic markers, changes in seismic stratigraphy, and were selected to capture the range of structures observed on the eastern Scotian Slope. Line drawings can be found at the end of the manuscript.

The water column in all type sections was depth-converted using a velocity of 1500 m/s. As such, the vertical scale bar for the water column is in meters (identified in blue text) whereas the vertical scale bar in the sub-surface is in seconds (twt; identified in black text). This correction significantly reduces velocity sags associated with deep seafloor canyons and removes the overall velocity sag on dip profiles associated with the seaward increase in water depth. Similarly, water-column velocities were depth-converted on all time-structure maps.

Seismic stratigraphic framework – eastern Scotian Shelf and Slope

Regional seismic horizons were correlated across the shelf and slope of the study area and were used to separate the stratigraphic succession into seven mega-sequences. The boundaries between these mega-sequences mark distinct phases in the seismic-stratigraphic evolution of the slope. Following a description of the basement architecture, we describe each mega-sequence (**MS**), including bounding horizon
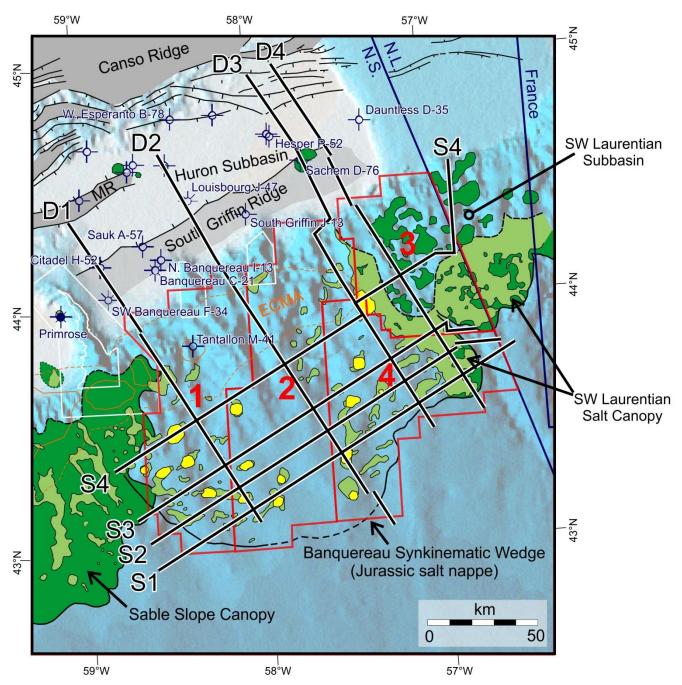
Figure 9. Key structural elements map in the primary study area. Location of representative dip lines (D1, D2, D3, D4) and strike lines (S1, S2, S3, S4) are shown. NS14-1 Parcels 1 to 4 are shown in red. Areas of thicker canopy salt shown in green. Salt diapirs that pierce the Banquereau Synkinematic Wedge and the overlying 'Missisauga fan comple' are shown in yellow. See text for details. Outline of eastern extension of ECMA shown in orange. MR = Missisauga Ridge. Some of the faults in the northern part of the figure are from Wade and MacLean (1990).

characteristics, sediment thickness distribution, seismic facies character, distribution and style of structures (including evidence for salt movement), and where possible the interpreted linkage to shelf depositional systems, including the location of shelf-edge trajectories. Except for MS-6, which encompasses about 60 Ma, most of the mega-sequences are believed to range from 10 to 35 Ma in duration, though there is considerable uncertainty about the age of strata in MS-1 and MS-2.

Basement structure

Key basement elements in the study area are shown on the time-structure map in Figure 13. The landward parts of the study area are dominated by two basement elements - a deep rift graben known as the Huron Subbasin (an eastern extension of the Abenaki and Sable subbasins), and a prominent basement high that borders it to the south, referred to as the South Griffin Ridge (SGR) (OETR, 2011; CNSOPB, 2013; Fig. 13). No clear basement marker is present below the Huron Subbasin on profiles D1 through D4 (Figs. 10, 11). Instead, a generally poorly imaged faulted interval is observed beneath its northern flank on all four type sections. Based on its faulted appearance and similarities in seismic facies to synrift clastics on the LaHave Platform, the interval is interpreted to correspond to a Triassic synrift succession beneath a deformed interval of autochthonous salt. The lack of impedance contrasts between synrift clastics and Meguma basement has previously been noted by Wade and MacLean (1990), and forces correlation of an approximate top-basement marker beneath the synrift package, increasing interpretation uncertainty. Similarly, no obvious seismic reflection defines the top of the South Griffin Ridge (SGR); rather, it is identified principally on the basis of patterns in sedimentary units in the Huron Subbasin adjacent to the SGR. The structural high appears to be asymmetric on time-migrated seismic profiles, with a steeper wall on its landward side that generally lacks coherent reflections, and a less steep seaward flank that shows subtle faulting. The weaker northeast continuation of the

ECMA is found about 30 km seaward of the SGR (Fig. 3); as such the SGR is located landward of the COB and probably corresponds to a large faulted horst block composed of continental crust. The elevated structure is likely veneered by salt expelled from the Huron Subbasin (Figs. 10, 11), but we emphasize that these interpretations are based on subtle seismic reflection patterns in a poorly imaged part of the seismic section on all four type profiles.

In the Call area southeast of the SGR, the top basement marker is increasingly reflective, showing a corresponding increase in rugosity towards deeper water on section D1, D2, and D3 (Figs. 10, 11). Nearest the SGR, one or two high amplitude reflections define the top basement surface, which has a smoother, generally low-relief topography offset only by minor undulations that may correspond to planar faults (Sibuet et al., 2012; see also Deptuck, 2011). The smoother basement character passes to the southeast, below and seaward of the BSW, into a highly rugose topographic surface with strong returns coming from one or two high impedance reflectors. The top basement surface is characterized by alternating peaks and troughs. In Figure 13, the sharp crests of these structural highs are identified by red dots and broader structures with multiple smaller peaks are identified by red lines. In general, the top basement surface gets shallower towards the south and southeast, where basement highs are generally broader. The "peaks" identified from one profile to the next commonly align, forming northeast-trending structures that can be continuous over distances of 20 to 40 km or more. Minor offsets are apparent along these structures and could have taken place across northwest-trending accommodation zones (transfer faults/fracture zones or relay ramps). These basement highs range in width from about 3 km to >7 km, with a maximum of 400 to 650 ms (twt) of relief relative to the immediately adjacent structural low. Using a conservative refraction velocity estimate of 5 km/s (from Funck et al., 2004), the maximum relief of these structures therefore ranges from 1.0 to 1.6 km. Internal reflections are generally
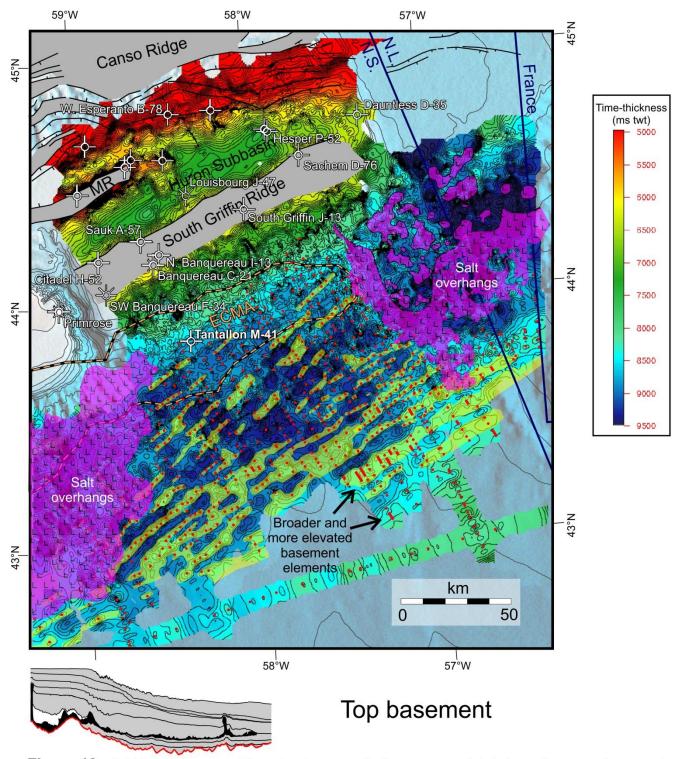
Figure 13. Gridded top basement time-structure map. Surface was correlated above the rugose basement that underlies the Scotian Slope and was correlated landward along the base of the autochthonous salt layer (top of the faulted synrift interval shown in profiles D1 to D4; Fig. 10). Red dots show the location of sharp top basement 'peaks' that appear to correspond to the corners of brittle, rotated fault blocks. Red lines identify profiles that cross broader basement elements. Yellow fill is an interpretation of the along strike alignment of basement highs. Pink shows areas of thick overhanging salt with diminished imaging. See text for details.
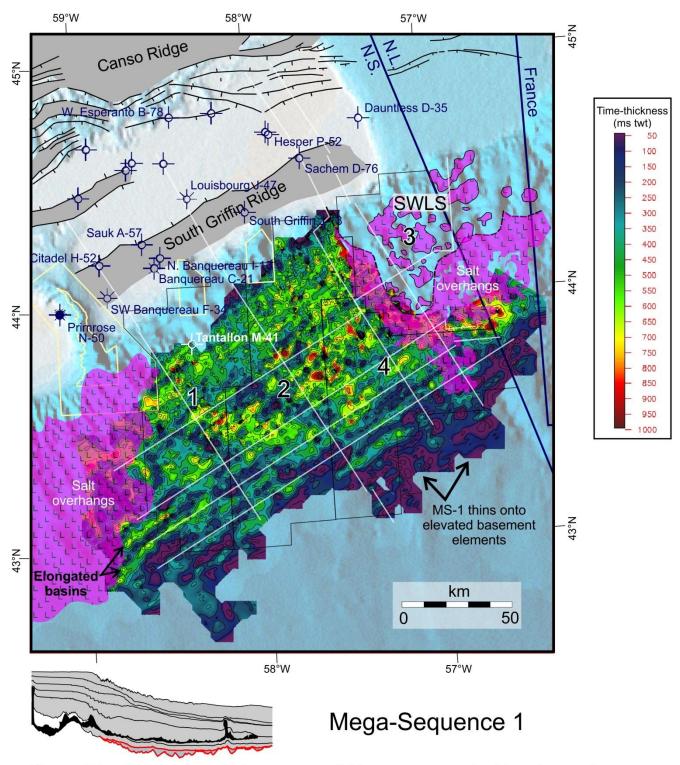
Figure 14. Gridded time-thickness map of Mega-sequence 1. Note the northeastern trending thicker basins that follow the trend of basement troughs between prominent basement highs. Pink overlay identifies areas of thicker overhanging salt. See text for details.

incoherent, but some internal layered reflections are apparent, particularly on reprocessed seismic profiles published in OETR (2011) (e.g. reprocessed TGS line 964-100 on Panel 6-4-1a).

Listric fault planes are well imaged between basement highs on some profiles, and appear to sole out along a common undulating – though variably imaged – surface. As such, the pointed crests of these northeast trending structural elements are interpreted to be the corners of highly rotated brittle fault blocks. They are particularly well imaged immediately south of The Gully, outboard the Sable Slope Canopy (Fig. 2). Fault offsets are dominantly towards the southeast. Because of the dominant northeast-southwest trend of these apparent fault blocks, type sections D1, D2, and D3, which are roughly normal to these features, provide the best imaging (Figs. 10, 11). The rugose top basement topography is much less clear on strike profiles, and it should also be noted that imaging of this surface is significantly affected by overlying salt stocks remaining within or above the BSW (e.g. velocity pull-ups on lines D1, D2, and S1, Figs. 10, 12a). Similarly, although the top basement surface has been correlated with moderate confidence below the seaward overhang of the SWLS salt canopy (e.g. profile D4), the top basement surface in the landward parts of the SWLS, has only been mapped with a low degree of confidence. Here, the presence of seaward leaning salt feeders and stepped counter-regional systems severely diminishes seismic imaging. Salt, however, appears rooted above the top basement surface, implying that profile D4 has crossed into an autochthonous or para-autochthonous salt basin (Fig. 11).

Mega-sequence 1 (MS-1) *– Early? to early Middle Jurassic (duration unknown)*
The highly rugose top basement surface described above was onlapped, and eventually overlain, by a generally low amplitude succession corresponding to MS-1 (Fig. 14). The J175 marker defines the top surface of MS-1, and corresponds to a somewhat diachronous boundary correlated across the slope region with moderate confidence. The marker separates low

amplitude onlapping and infilling reflections below from generally higher amplitude continuous draping reflections above. MS-1 is only recognized on the slope, seaward of the SGR (underlying Parcels 1, 2, and 4). Correlation uncertainty of the J175 marker increases towards the northeast, towards the SWLS and Parcel 3. The age of the J175 surface, and underlying MS-1 deposits, is uncertain.

Thickness maps between the top basement surface and J175 indicate that MS-1 forms a number of narrow, northeast trending basins that are up to 700 ms (twt) thick immediately above the elongated axes of underlying basement lows (i.e. the troughs between basement highs) (Fig. 14). MS-1 deposits thin abruptly above the pointed crests of underlying fault blocks. Subtle along-strike offset of the thickest parts of these narrow elongated basins is common, and largely reflects offsets in the underlying basement structures. More regional thickness patterns are also evident. The landward termination of MS-1 is interpreted to thin and onlap the southeastern flank of the SGR or the smoother basement rocks immediately adjacent to it, as seen on profiles D1, D2 and D3. However, poor seismic imaging and potential faults in this area, increase the uncertainty of this interpretation. Further seaward, MS-1 also thins and onlaps the broader, elevated basement elements in the southern and southeastern most study area, as seen on profiles D3 and D4 (Fig. 11) and on time-thickness maps (Fig. 14).

A few normal faults extending up from the crests of basement highs appear to offset strata below and above the J175 marker, but there are no indications that the basement was actively deforming during sedimentation of MS-1. Instead, the unit appears to have more passively filled and smoothed over pre-existing topographic relief along the top basement surface, with a few normal faults developing later in response to compaction or minor basement adjustments.
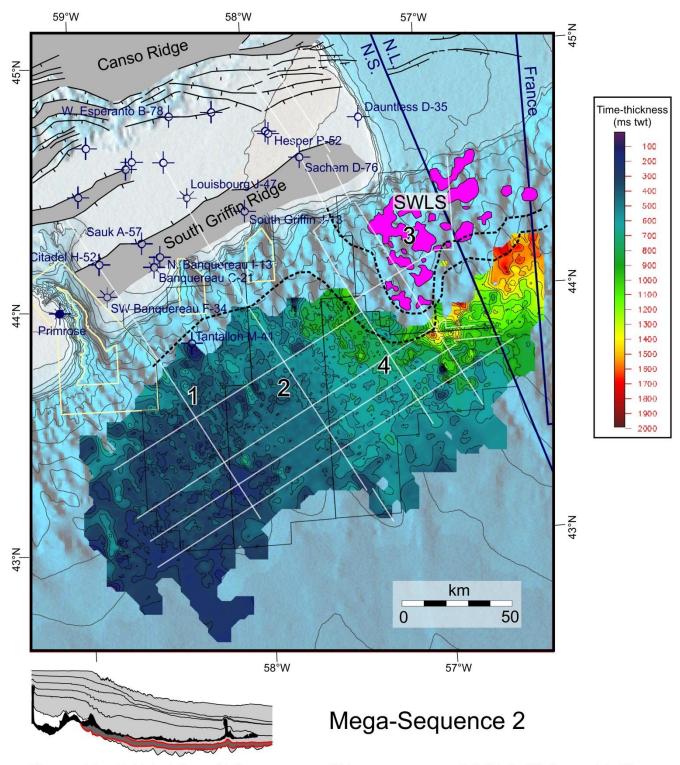
Figure 15. Gridded time-thickness map of Mega-sequence 2 (Middle(?) Jurassic). Note the overall decrease in thickness away from the southwestern Laurentian Subbasins (SWLS). MS-2 records the first pulse of clastics to build out towards the eastern Scotian Slope. Dashed lines identify the J175 and J163 salt contacts. See text for details.

Mega-sequence 2 (MS-2) – Middle Jurassic (duration unknown, but probably <11 Ma)

MS-2 forms a wedge-shaped deposit that is thickest along the northeastern slope outboard salt canopies expelled from the SWLS (e.g. northern part of Parcel 4); it is thinnest in Parcel 1 towards the southwest, approaching the Sable Slope Canopy (Fig. 15). The general sediment thickness pattern is clearly shown along profiles S1, S2, and S3 (Fig. 12a, 12b). Its lower boundary is the J175 marker described previously, and its upper boundary is the J163 marker (OETR, 2011) – a somewhat diachronous Middle Jurassic (intra-Callovian) marker that is roughly equivalent to the Scatarie limestone on the shelf (Weston et al., 2012; Fig. 4) and the J2 marker in the Sohm Abyssal Plain (Ebinger and Tucholke, 1988; Wade et al., 1995). MS-2 in many places corresponds to an abrupt increase in reflection amplitude. Some relatively continuous markers within this interval produce very strong reflections that probably correspond to carbonates or even volcanics. The reflection character is increasingly mixed towards the southwest Laurentian salt canopy, where MS-2 is 900 ms (twt) thick and terminates along a salt contact along the southwest edge of the Laurentian Subbasin (Fig. 15). Imaging of MS-2 diminishes substantially below thicker intervals of allochthonous salt, with significant velocity pull-ups increasing correlation uncertainty. Still, MS-2 appears to be thickest (up to 1400 ms twt) below the most easterly salt sheets in the study area (e.g. profile D4, Fig. 11). MS-2 diminishes to just 250 ms (twt) thick in the southwestern study area.

Like MS-1, MS-2 cannot be confidently correlated landward onto the shelf or into the SWLS. Although no direct correlation is possible, on the basis of stratigraphic position MS-2 and perhaps MS-1(?) on the slope are interpreted to be roughly equivalent to the interval between the J163 marker and the top of the autochthonous salt in the Huron Subbasin. This succession on the shelf consists of poorly imaged faulted strata that are thickest along the axis of the Huron Subbasin. Accommodation for these strata was provided by salt expulsion. Poorly imaged offlap breaks

associated with the Mohican Formation (Toarcian? to Bajocian) are recognized locally, particularly towards the northeastern study area (see figure 5.6 of CNSOPB, 2013), but in general seismic imaging in this succession is too poor to make any definitive seismic-facies-based interpretations.

Salt contacts indicate salt rose sub-vertically out of the SWLS, flowing towards the southwest, south, and southeast as MS-2 strata aggraded seaward of the advancing salt front. The salt contact at the top of MS-2 (along the J163 marker) is located roughly 10 to 15 km ahead of the salt contact at the base of MS-2 (along the J175 marker) (Fig. 16). Strata within MS-2 also appear to terminate along poorly imaged salt contacts located along the southern flank of the SGR. Assuming that the SGR once formed the seaward depositional limit of the autochthonous salt basin, the salt front migrated seaward about 45 km by the end of MS-2 (though much of this may have taken place in the latter parts of MS-2). This indicates that salt expulsion from the Huron Subbasin, across the southern flank of the SGR, was at least partly contemporaneous with salt inflation and expulsion from the SWLS.

Mega-sequence 3 (MS-3) – Middle to Late Jurassic (duration ~ 19 Ma)

MS-3 is a structurally complex interval on the slope that records the co-development of a large salt nappe across the southwestern study area below parcels 1, 2, and 4 (corresponding to the BSW of Shimeld, 2004; Ings and Shimeld, 2006) and a poorly constrained stepped counter-regional salt expulsion system to the east below Parcel 3 (corresponding to the SWLS) (Fig. 9). Type section S4 nicely illustrates the cross-slope transition between these two salt tectonic domains, as does a comparison of dip profiles D1, D2, or-D3 with dip profile D4 (Figs. 10, 11, 12b). The lower boundary of MS-3 corresponds to the intra-Callovian J163 marker described previously (Fig. 4). Its upper boundary is our J152 marker located just below the top of the Jurassic succession on the shelf (calibrated by several outer shelf wells, and approximately one seismic loop deeper than the J150 marker of OETR, 2011). The J152 marker was
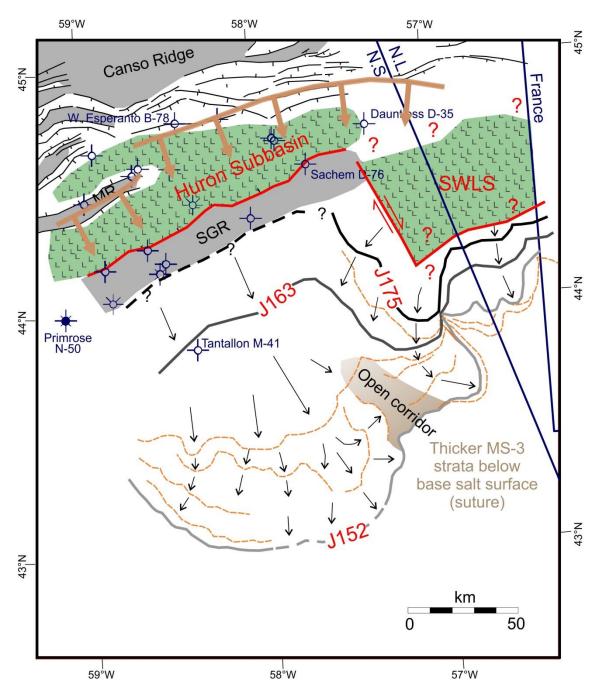
Figure 16. Key structural elements map in the primary study area, draped by salt contacts for the J175, J163 and J152 markers. Also shown is a highly schematic estimates of the original autochthonous salt basins (green fill) and several intermediate salt contacts (orange dashed lines). Brown arrows indicate the progradation direction immediately above the J163 marker along the landward margin of the Huron Subbasin. Two salt basins supplied allochthonous salt into the NS14-1 Call area. Black arrows show the interpreted trajectory of the advancing allochthonous salt front (salt expulsion vectors). See text for details.

correlated with moderate to high confidence onto the slope *above* the BSW, where it corresponds to a high amplitude reflection.

Because part of MS-3 was deposited above an allochthonous salt nappe on the slope, at the same time sediment accumulated outboard of the seaward advancing salt front, a repeated section is generated above and below the allochthonous salt layer or its equivalent weld. As such, three separate time-thickness maps are used to show the distribution of MS-3 strata. Figure 17 shows the time-thickness of MS-3 strata between the J152 marker and the top-allochthonous salt surface (or the equivalent weld) on the slope (i.e. MS-3 strata within the BSW). Figure 18 shows the time-thickness of MS-3 strata below the base-allochthonous salt surface (or the equivalent weld) but above the J163 marker on the slope (i.e. MS-3 strata beneath the BSW). Figure 19 shows the total time-thickness of MS-3 by adding the first two maps together, plus the thickness between the J152 and J163 markers on the shelf.

In contrast to the base salt surface that forms a prominent high amplitude trough, the top of the allochthonous salt layer commonly does not produce a distinctive high amplitude reflection, making it difficult to distinguish allochthonous salt from overlying low-amplitude strata. Recognition of subtle reflections within minibasins and turtles, combined with the use of several different on-the-fly post-stack filtering options, allowed us to correlate a top salt surface beneath the BSW with moderate confidence. Preserved salt within the nappe is dominantly in the form of rollers and pillows, but salt stocks and walls are increasingly common nearing the seaward termination of the BSW. The time-thickness between the base and top salt surfaces in the BSW was excluded from all three maps (i.e. remnants of salt within the BSW are not included in the time-thickness maps). Salt that is thicker than 500 ms (or roughly 1.1 km using 4400 m/s salt velocity from Shimeld, 2004) within the BSW is identified in Figure 17.

MS-3 above the allochthonous salt nappe and in the SWLS

On the slope, the BSW forms a prominent seaward-tapering wedge that is up to 2400 ms (twt) thick on the upper slope, thinning to < 500 ms thick on the lower slope, above the inflated seaward termination of the allochthonous salt layer (Fig. 17). A series of normal listric faults offsets the J152 marker immediately above the SGR (Fig. 20), across a region of poor seismic imaging. The faults sole out in allochthonous salt that was expelled from the Huron Subbasin during MS-2, with some seismic profiles indicating that large salt rollers still remain in the headward part of the BSW, above the seaward flank of the SGR (e.g. profiles D1 and D2; Fig. 10). Further down the slope, strata within the BSW show local thinning coincident with the thickest salt bodies. Seismic facies consist primarily of alternating intervals of high amplitude, continuous reflections and lower amplitude reflections. Salt-related structures down-slope from the SGR are complex, ranging from landward dipping sigmoidal reflections as described by Ings and Shimeld (2006, their figure 5), to roho systems with numerous listric faults that sole-out into the salt detachment (e.g. profile D3), and turtle structures (profiles S2, D1-D3). In some locations excessive rotation along listric faults, coupled with minor amounts of shortening, generated subtle folds with overthrusting (e.g. profiles D3 and S3; Figs. 11, 12b). Some shortening also appears to be recorded by thrust sheets immediately down-slope from the extensional faults at the head of the BSW (e.g. profile D2). Listric faults within the BSW are complex, and do no strictly record extension that takes place in the down-slope direction (relative to the modern slope) (Ings and Shimeld, 2006). Profiles S2 and S3 for example cross a 40 km long extensional fault zone that soles out along a north to northwest oriented chain of salt bodies (Fig. 20). The extension direction in this case is towards the southwest, perpendicular to the extension direction recorded by listric faults in the headward parts of the BSW.
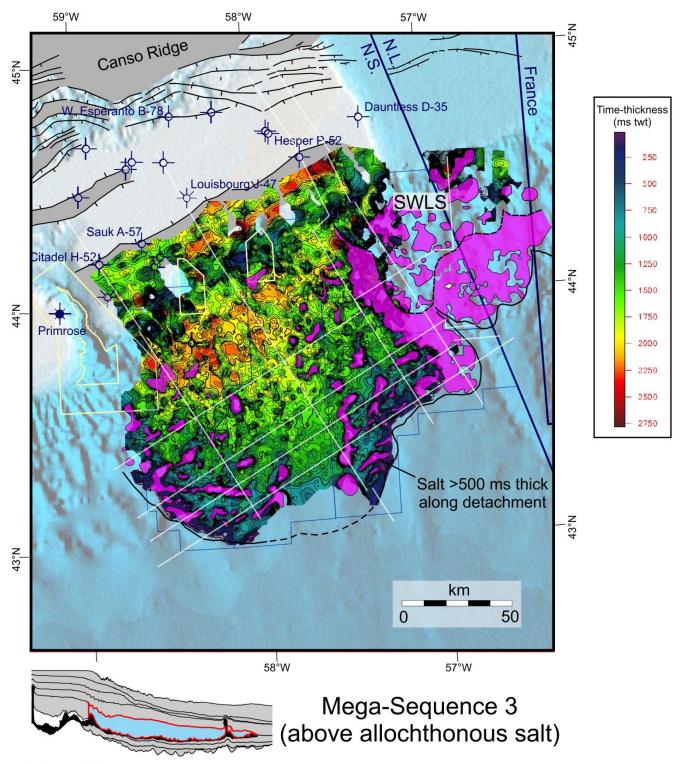
Mega-Sequence 3
(above allochthonous salt)

Figure 17. Gridded time-thickness map of the upper parts of Mega-sequence 3 (Middle to Late Jurassic) found above the top allochthonous salt surface, but below the J152 marker. Note the overall seaward-tapering wedge-shaped geometry of the Banquereau Synkinematic Wedge. Salt along the base of the detachment surface exceeding 500 ms (twt) is identified by pink fill. Also shown in pink are areas of thicker salt associated with the southwest Laurentian Subbasin (SWLS).
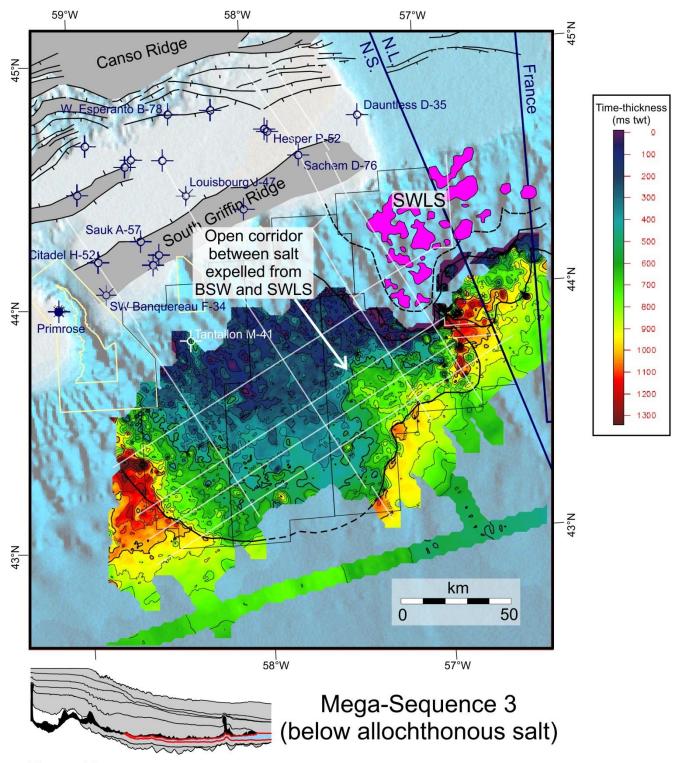
Figure 18. Gridded time-thickness map of the lower parts of Mega-sequence 3 found below the base allochthonous salt surface, but above the J163 marker. Strata in this interval were deposited while the Banquereau Synkinematic Wedge advanced seaward, as salt was expelled from both the Huron and southwest Laurentian subbasins. The ridge of thicker sediment in the eastern part of the BSW accumulated along an open corridor between the two advancing salt sheets.
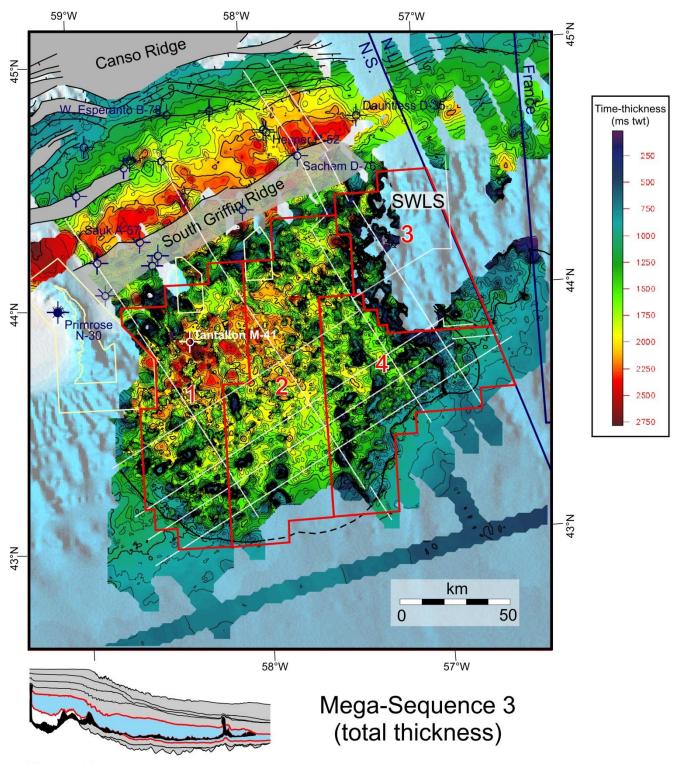
Figure 19. Gridded time-thickness map of Mega-sequence 3 (Middle to Late Jurassic) between the J163 and J152 markers. Note that the thickness of salt remaining along the basal detachment surface of the Banquereau Synkinematic Wedge is not included in this time-thickness map.

In contrast to the prominent listric faults that offset the J152 marker all along the landward parts of the BSW, the J152 marker southeast of Sachem D-76 and Dauntless D-35 terminates along a series of seaward leaning salt welds associated with a complex stepped counterregional salt expulsion system in the landward parts of the SWLS (Parcel 3; see profiles D4 and S4; Figs. 12b, 13). The BSW does not exist here, and it is not possible with existing data to correlate MS-3 through this region. Salt feeders are complex and at least three tiers of salt overhang potential MS-3 stratigraphic intervals on some seismic profiles, significantly diminishing seismic imaging. Still, recognition of seismic reflections between some salt feeders and correlation of MS-3 below the expelled salt canopies seaward of the SWLS (e.g. seaward part of profile D4 (Fig. 11), indicates that MS-3 minibasins in some form should be present within the SWLS.

MS-3 below the salt nappe
MS-3 below and seaward of the BSW has been correlated with a moderate to high degree of confidence. Seismic imaging below the salt detachment surface is moderate to poor. Where there are no salt overhangs seaward of the BSW, imaging is excellent. Like the succession above the allochthonous salt, seismic facies are dominated by alternating continuous high amplitude reflections and low to moderate amplitude reflections. Reflections are generally parallel (layer-cake) and unfolded, broken only by a few small-offset normal faults out on the Sohm Abyssal Plain. Reflections terminate in the landward direction against the base salt contact (profiles D1, D2, and D3; Figs. 10, 11). MS-3 ranges from less than 200 ms (twt) thick beneath the northern and central parts of the BSW and towards the SWLS, to a maximum thickness of about 1400 ms (twt) near the lateral and seaward limits of the BSW (Fig. 18). Further seaward, MS-3 tapers gradually to less than 700 ms (twt) thick on the Sohm Abyssal Plain in the southeastern parts of the study area.

A 15 to 35 km wide and 45 km long ridge of thicker sub-salt sediment is present below the eastern half of the BSW (Fig. 18). Profile D3 crosses this sub-salt sediment

ridge obliquely, showing a more abrupt vertical salt climb than is observed on profiles D1 and D2. The ridge defines a boundary between two advancing salt fronts – one coming from the seaward flank of the SGR (western and central parts of the BSW) and the other from the western margin of the SWLS (Figs. 16, 18). The convergence of these salt fronts probably formed a salt suture above the sub-salt sediment ridge, with salt from both areas forming part of the BSW detachment surface (discussed in more detail in a later section).

MS-3 on the shelf
On the shelf landward of the BSW, MS-3 sedimentation was focused along the axis of the Huron Subbasin, where up to 2300 ms (twt) of Mic Mac and equivalent strata were deposited immediately adjacent to, and above, the SGR (Fig. 21). Accommodation space was provided through salt expulsion. The onset of MS-3 on the shelf records an abrupt change in the seismic stratigraphic response immediately above the J163 marker. Early sedimentation was focused along clearly defined prograding clinoforms capped by a toplap surface. This initial Callovian to Oxfordian pulse of mixed siliciclastics (calibrated at West Esperanto B-78) forms a southeastward thickening wedge that extends all along the northern rim of the Huron Subbasin (e.g. northernmost part of profiles D3 and D4 – Fig. 11, and shelf-edge trajectory 1 on Fig. 21). In the center of the Huron Subbasin where this interval is thickest, internal reflections are poorly defined and cannot be correlated over long distances. It passes up-section into a mixed aggradational-progradational system consisting of more continuous alternating and generally parallel high and low amplitude reflections that terminate in a complexly faulted region adjacent to and above the SGR. Two distinct shelf-edge inflection trends are recognized on seismic profiles (shelf-edge trajectories 2 and 3 on Fig. 21). These record the southeastward advance of clastics and carbonates in the Oxfordian to Tithonian, immediately upslope from the BSW. Several wells penetrate the upper parts of MS-3 above the SGR. Louisbourg J-47 encountered over 1800 m of Upper Jurassic strata dominated by thick intervals of tight,
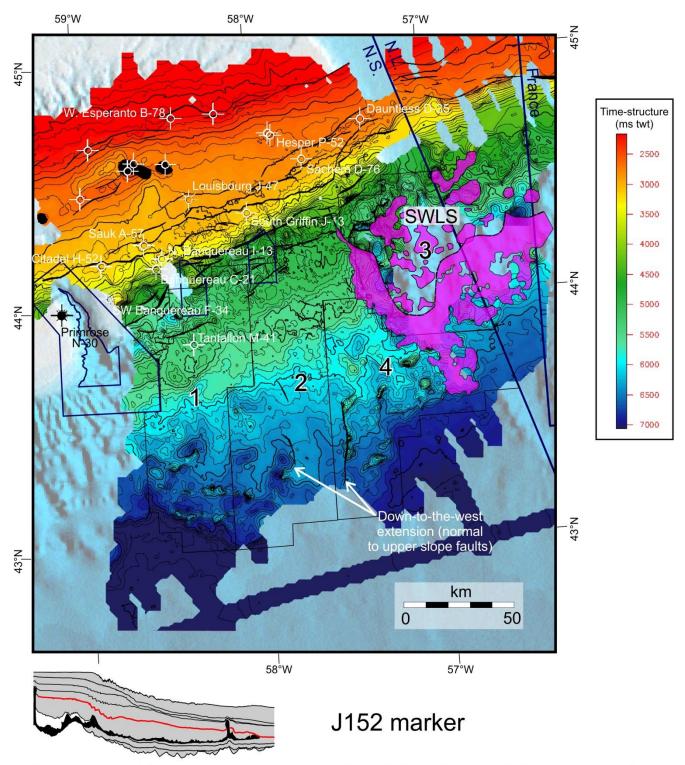
Figure 20. Gridded time-structure map of the J152 marker that defines the boundary between MS-3 and MS-4. Normal faults are identified in black.
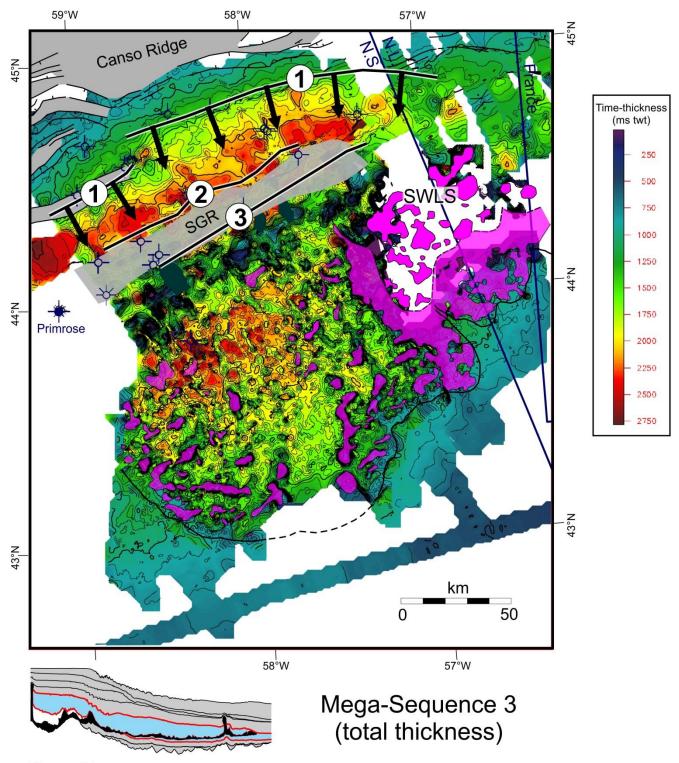
Mega-Sequence 3
(total thickness)

Figure 21. Annotated time-thickness map of MS-3, showing the location of shelf-edge trajectories 1, 2, and 3 that document the seaward advance of mixed clastics and carbonates of the Mic Mac Formation as the shelf delivery systems prograded and aggraded across the Huron Subbasin and South Griffin Ridge (SGR). Seaward advance of these shelf-edge systems began immediately above the J163 marker (1) and ended at the J152 marker (3) in the latest Jurassic. They were the primary source of sediments (carbonates and clastics) supplied to the Banquereau Synkinematic Wedge in the Callovian to Tithonian.

marly, micritic and oolitic limestones, with thinner interbedded delta front and shallow marine sands. South Griffin J-13 encountered a similar Upper Jurassic succession with more than 1300 m of alternating shallow marine sandstones and carbonates.

Mega-sequence 4 (MS-4) – *Latest Jurassic to Aptian (duration ~ 34 Ma)*

MS-4 marks an abrupt change in the distribution of sediments on the shelf and slope (Fig. 22), with a corresponding change in seismic facies character (Fig. 23; described below). The lower boundary of MS-4 is the J152 marker described in the previous section. Its upper boundary is our K112 surface that, rather than corresponding to a distinct seismic reflection, instead corresponds to a regionally important seismic facies boundary on the slope (described in the following section). This boundary, which we anticipate will be somewhat diachronous, ties to the base of an Early Albian interval at Tantallon M-41 on the upper slope (OETR, 2011). Seismic correlation into equivalent shelf strata is difficult, owing to the absence of distinct reflectors and the presence of growth faults, but the time-equivalent surface is probably found near the top or slightly above the Naskapi Member on the outer shelf (generally latest Aptian; Weston et al., 2012). As such, MS-4 on the slope is equivalent of the Missisauga and the lowermost Logan Canyon formations on the shelf (Fig. 4).

On the shelf, the transition from MS-3 to MS-4 takes place across the J152 marker that defines an important boundary separating parallel reflections below from divergent or onlapping reflections above. The discordance across this boundary is particularly well defined on the landward parts of profiles D3 and D4 (Fig. 11), which cross the southwestern flank of the Avalon Uplift (Fig. 2). MS-4 thins abruptly to the northeast and this pattern reflects the onlap and thinning of MS-4 strata onto the up-arched J152 marker (Fig. 22). In contrast to MS-3, little accommodation formed above the Huron Subbasin during MS-4. Instead, MS-4 forms a seaward-thickening wedge and the thickest shelf deposits are noticeably shifted to the

southwest, where the Huron Subbasin transitions into the Sable Subbasin (immediately outboard the Missisauga Ridge). MS-4 is about 1000 ms (twt) thick here (Fig. 22). Several wells penetrate MS-4 on the shelf, where they encountered a Lower Cretaceous succession of porous fluvial-deltaic sandstones of the Missisauga Formation above and below an interval of oolitic limestones referred to as the O-marker, and capped by Naskapi Member shales (Wade and MacLean, 1990; Fig. 4).

Shelf-edge trajectories in MS-4 are difficult to identify, but a trend of subtle offlap breaks has been correlated immediately above the seaward edge of the SGR within the lower part of MS-4 (shelf-edge trajectory 4; Fig. 22). Seaward of the SGR, MS-4 is thickest in two areas – on the upper slope in the western study area (in Parcel 1) and in the landward parts of the SWLS in the eastern study area (in Parcel 3). In the western study area, it reaches a maximum time-thickness of 2100 ms (twt) across a series of northeast trending outer shelf listric growth faults that sole out in the salt detachment below the BSW. Here, a thickened lens of strata above the O-marker (K-130 marker) is largely responsible for the overall thickness increase (e.g. profiles D1 and D2), though some growth also took place earlier, seaward of shelf-edge trajectory 4. Shelf-edge trajectory 5 is tentatively placed along the trend of this heavily faulted Upper Missisauga equivalent lens (Fig. 22), which we interpret as a shelf-edge delta.

Missisauga fan complex

On the slope, the transition from MS-3 to MS-4 takes place across a complex interval immediately above the J152 marker, but below a prominent unconformity (Fig. 23). The seismically identified slope unconformity has not been calibrated by a well, but its stratigraphic position is consistent with the near-base Cretaceous Unconformity (NBCU) described by Weston et al (2012). As such, the interval between the J152 marker and this erosive surface may record the complex stratigraphic response on the slope to the Avalon Uplift on the shelf. The unconformity is particularly well imaged above the eastern and seaward parts of the BSW, where it forms a
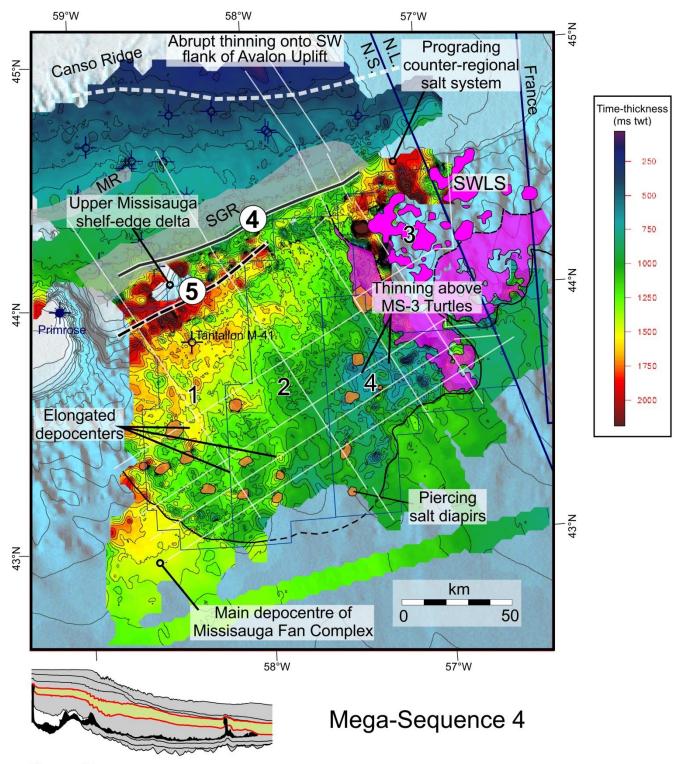
Figure 22. Gridded time-thickness map of Mega-sequence 4 (latest Jurassic to Aptian). Note the thinning towards the southwest flank of the Avalon Uplift, and the overall southwesterward shift in the thickest shelf deposits. Also note that there is no longer any detectable down-building into the Huron Subbasin. The thickest sediments are found seaward of shelf-edge trajectories 4 and 5 where the Missisauga fan complex was deposited above and adjacent to the Banquereau Synkinematic Wedge. Piercing diapirs are shown in orange. See text for details.

series of 3 to 5 km wide curvi-linear canyons separated by 4 to 13 km wide down-slope elongated erosional remnants. The erosional remnants are up to 400 ms thick (twt) and contain broad high amplitude and continuous peaks and troughs on the lower slope, with increasingly common lower amplitude reflections moving up the slope. Locally, more than one erosive surface is evident above these features on the upper slope. The erosional remnants are highlighted in grey on the type profiles (Figs. 10, 11, 12a, 12b).

Above the erosional remnants, MS-4 is dominated by more discontinuous seismic reflections (Fig. 23). Aside from a discontinuous higher amplitude reflection interval in the upper parts of MS-4 (roughly the slope equivalent of the O-marker or K130) seismic reflections cannot be correlated with confidence over distances that exceed 15 to 20 km. Local erosive surfaces are apparent, but in contrast to the unconformity near the base of MS-4, cannot be correlated regionally. Intervals of low amplitude reflections commonly have wedge-shaped geometries that border discontinuous brighter amplitude reflections. Well-developed shingling is common, particularly in higher amplitude seismic reflections. So too are intervals of chaotic high and low amplitude reflections. Some U-shaped high amplitude reflections stack vertically or laterally between wedge-shaped lower amplitude intervals, resembling the migrating channel-forms described in detail by Deptuck et al. (2003, 2007) and others. These seismic facies are consistent with curvi-linear to sinuous sand-prone submarine channels that stack and migrate between muddy levees. Low amplitude reflections are generally more continuous than the high amplitude reflections, but some continuous (over distances of 15 to 20 km) high amplitude reflections are also found along the bases of some channel-levee systems. These resemble more widespread sheet sands associated with channel-levee avulsions. On dip profiles, higher amplitude seismic facies are more continuous but a subtle shingling of reflections is still common. This implies that dip lines are crossing the length axis of largely channeled turbidite corridors. It is possible to map

some of these leveed channel complexes even on 2D seismic data.

This interpreted submarine fan succession is referred to herein as the "Missisauga fan complex" (Fig. 23). It has only been calibrated by one well in the study area - Tantallon M-41. Two conventional cores are available from this well in MS-4. The shallowest core is in slope strata equivalent to the Upper Missisauga Formation, < 20 km seaward from a proposed Upper Missisauga shelf edge (shelf-edge trajectory 5, Fig. 22). It contains evidence for mass wasting with shear zones, ductile deformation, and blocks of failed material (see Piper et al., 2010), which is not surprising given its proximity to the Upper Missisauga shelf edge. The deepest core is through slope strata equivalent to the Lower Missisauga Formation (using the two-member division of Welsink et al., 1989), located about 42 km seaward of shelf-edge trajectory 4 (Fig. 22). The core shows the presence of numerous sharp-based thin-bedded turbidites composed of very fine grained to medium-grained sandstone (see Piper et al., 2010), including turbidites consistent with fine-grained overspill from levees (e.g. Piper and Deptuck, 1997).

The Missisauga fan complex is up to 1800 ms (twt) thick southwest of the underlying BSW. Above the BSW, the fan complex shows a general decrease in thickness from the west to the east across Parcels 1, 2, and 4 (compare profiles D1 and D3; Figs. 10, 11). In detail, several finer-scale thickness variations are apparent above the BSW. Late salt deflation below, or extension within, the BSW appears to have created accommodation space for several 10 to 20 km wide down-slope elongated depocenters, particularly above the western half of the BSW (Fig. 22). Similarly, rim synclines appear to have formed along isolated salt stocks that extend up from the underlying salt nappe, piercing MS-4 strata. These indicate active salt movement on the slope during MS-4. Inverted MS-3 turtles along the easternmost parts of the BSW appear to have formed positive-relief bathymetric elements that coincide with elongated thins within MS-4 slope stata (e.g. eastern part of profile S2 and S3; Fig. 12a, 12b). Several additional

Figure 23. Close-up of profile S3 showing the sharp contrast in seismic facies between MS-3 and MS-4, and the seismic facies typical of the Missisauga fan complex. Discontinuous to shingled higher amplitude seismic facies, interpreted to correspond to migrating submarine channels, are highlighted in yellow. They are commonly flanked by wedge-shaped deposits interpreted as submarine levees. Orange identifies potential sheet or channeled-sheet sands deposited after periods of channel-levee avulsions.

structures deform MS-4 strata on the slope. For example, broad folds are present on the upper slope, particularly obvious in profile D1, and a series of salt-cored folds is present on the lower slope (e.g. profiles D3, S1 and S2) (Figs. 11, 12a). There is no obvious thinning of MS-4 strata above these folds, indicating that folding post-dates the Missisauga fan complex. These folds are discussed in more detail in a later section.

MS-4 in the SWLS

In the eastern study area (Parcel 3), MS-4 thickens to the southeast where sediment progradation expelled salt from the landward parts of the SWLS. MS-4 reflections terminate in a quasi downlap fashion onto seaward leaning salt welds (e.g. profiles D4 and S4, Figs. 11, 12b) to produce well-defined expulsion rollovers (Hudec and Jackson, 2011). Seaward of these expulsion rollovers, salt contact maps indicate that the salt from the SWLS was actively being expelled during MS-4 producing an amalgamated canopy landward that passes into overhanging salt sheets to the southeast, to form the Southwest Laurentian Salt Canopy (Fig. 9). MS-4 strata accumulated in a series of minibasins above this amalgamated salt canopy (lines D4, S4; Figs. 11, 12b).

Mega-sequence 5 (MS-5) *– Albian and Cenomanian (duration ~ 19 Ma)*

The onset of MS-5 is marked by an abrupt seaward shift is shelf sedimentation above the Naskapi Member of MS-4, with a corresponding abrupt decrease in reflection character on the slope above the Missisauga fan complex. Its lower boundary is the earliest Albian K112 surface described in the previous section. Weston et al. (2012) identified a maximum flooding surface located near the Aptian/Albian boundary (near the top of the Naskapi Member), which we interpret as the base of MS-5 on the shelf. Its upper boundary is the K94 marker that roughly corresponds to the base of the Petrel Member of the Dawson Canyon Formation (see Wade and MacLean, 1990). As such, MS-5 is time-equivalent to the Logan Canyon Formation (minus the Naskapi Member) and the lower half of the Dawson Canyon Formation (Fig. 4).

A notable feature of MS-5 is the sharp contrast in the thickness of outer shelf versus slope sediments (Fig. 24). Much of the outer shelf during MS-5 was located seaward of the SGR, on the present-day upper slope. Significant growth took place in the landward parts of Parcels 1 and 2, across a series of northeast-trending normal faults located seaward of the SGR (Fig. 25, 26). MS-5 increases in time-thickness from about 700 ms (twt) above the SGR, to over 1200 ms (twt) across these faults. The thickest part of this MS-5 shelf-margin system is 18 to 25 km wide and forms a linear northeast-trending thickness anomaly that can be followed along strike for more than 120 km. These outer shelf deposits record a complex stratigraphic history with two clear cycles of aggradation, followed by erosional truncation, and followed in turn by progradation of clinoforms (e.g. profiles D1, D2 and D3 in Figs. 10, 11). Although no wells penetrate the thickest outermost shelf parts of MS-5, several wells have sampled alternating intervals of shale and sandstone in more landward positions. Overall the log motifs are serrated, but numerous stacked 10 to 30 m thick sandstone intervals in Sachem D-76, South Griffin J-13, Louisbourg J-47, and SW Banquereau F-34, have blocky to regressive log motifs that alternate with 5 to 50 m thick shale intervals. Sands are particularly well developed immediately above the Naskapi Member, within the Cree Member of the Logan Canyon Formation (Fig. 4). We tentatively correlate these sands with the lower interval of progradation in MS-5, with the younger period of progradation tentatively tied to the sandy Marmora Member of the Logan Canyon Formation (see Wade and MacLean, 1990).

The youngest and seaward most clinoforms of MS-5 are commonly eroded by a prominent unconformity or are capped by a highly deformed interval where numerous detachment faults in younger strata sole out. The maximum regression of the margin, in post-Triassic times, was achieved during MS-5, and we place a Late Albian to Cenomanian shelf-edge trajectory just landward of Tantallon M-41, in present day water depths that exceed 1000 m (Fig. 25).
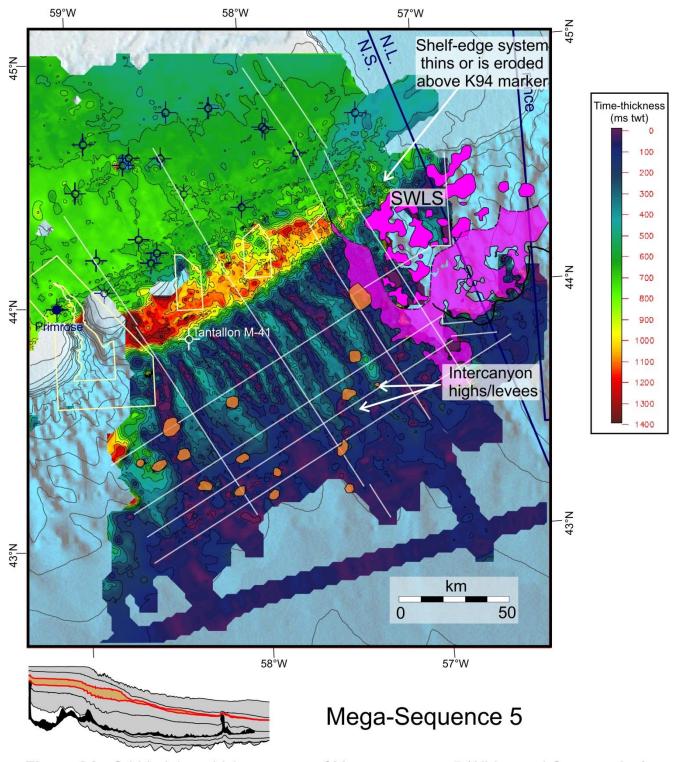
Figure 24. Gridded time-thickness map of Mega-sequence 5 (Albian and Cenomanian). Note the sharp contrast in thickness of outer shelf versus slope deposits. MS-5 records the transition to a bypass slope, with little reservoir potential on the slope.
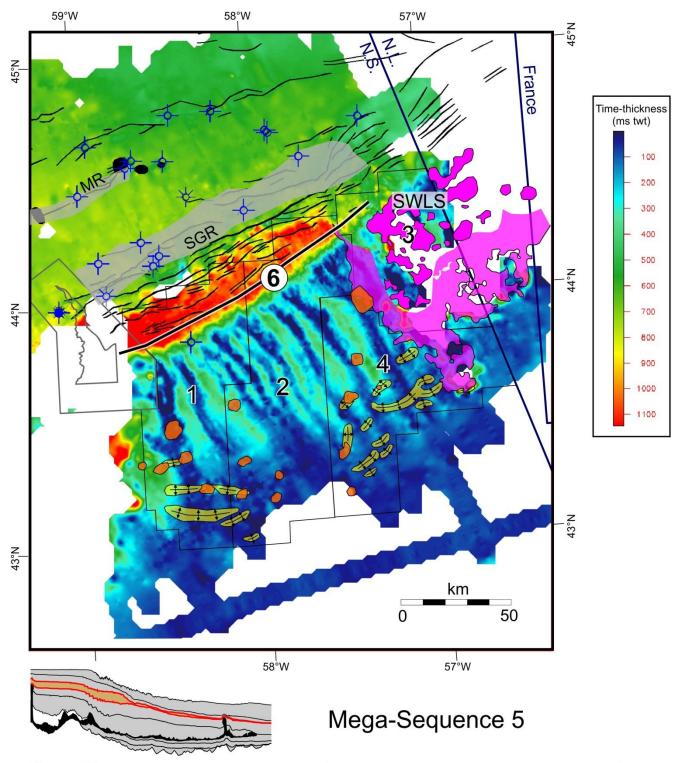
Figure 25. Annotated time-thickness map of Mega-sequence 5 overlain by listric normal faults on the outer shelf and showing the location of salt-cored folds along the toe of the Banquereau Synkinematic Wedge. The folds grew during MS-5, inverting turbidite-bearing strata of MS-4 (Missisauga fan complex). The distribution of pierced salt diapirs is shown in orange. Shelf-edge trajectory 6 represents the maximum regression of the margin. See text for details.
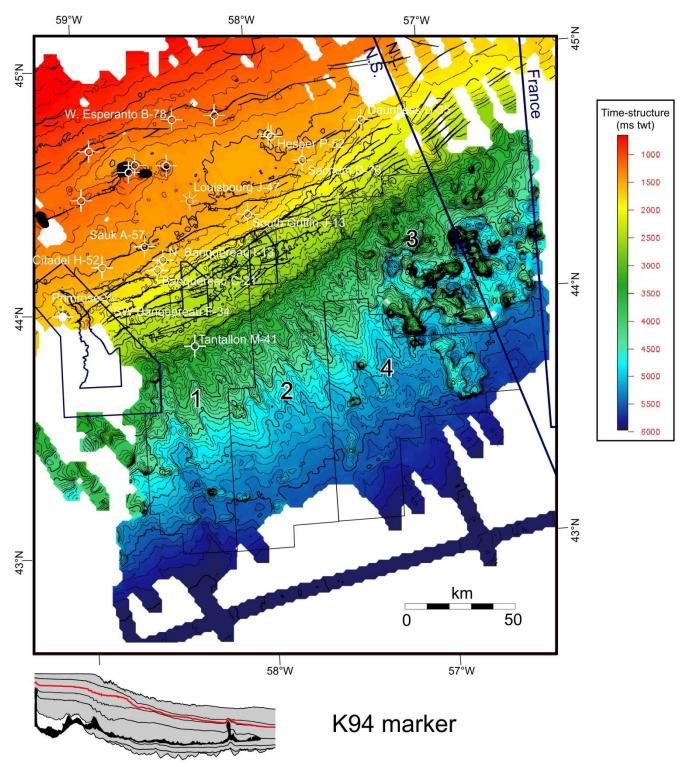
Figure 26. Gridded time-structure map of the K94 marker (near base Petrel marker).

Shortland fan complex

Unlike MS-4 that is characterized by a mix of high and low amplitude reflections on the slope, MS-5 is characterized by distinctly low amplitude to transparent seismic facies with subtle wavy internal reflections (Fig. 23). Tantallon M-41 penetrated the toe-sets of seismically recognized clinoforms located < 5 km seaward from a proposed Albian shelf edge (shelf-edge trajectory 6, Fig. 25). The well encountered principally fine-grained deposits, with a 23.5 m long conventional core containing ample evidence for mass wasting (Piper et al., 2010). Given its location relative to the steep shelf edge, evidence for mass wasting is not surprising. Seaward of the well location, the transition from MS-4 to MS-5 records a significant reduction in the amount of sediment stored on the slope, and a significant change in the architecture of slope deposits. Time-thickness maps indicate that MS-5 consists of a series of 3 to 15 km wide downslope elongated sedimentary ridges that separate numerous 2 to 8 km wide canyons west of the SWLS (Fig. 25). The ridges, which are up to 550 ms thick, can be tracked from the base of the Albian-Cenomanian clinoforms for 90 to 110 km down the slope. They form downslope thinning wedges on dip profiles that pass through their thickest parts (e.g. profile D1; Fig. 10). Coincident with their downslope decrease in relief, canyons between ridges become broader and gradually merge with adjacent canyons to form a largely erosive lower slope. On the basis of their wedge-shaped external form and their low amplitude seismic response, these ridges are interpreted as mud-prone levees that formed from the overspill of fine-grained turbidites.

We refer to this network of empty canyons flanked by muddy levees as the Shortland fan complex. The transition from the Missisauga fan complex below to the Shortland fan complex above is marked by the onset of intense slope bypass, with distinctly non-aggradational canyon floors. With the exception of the intercanyon highs/levees, little sediment appears to have been stored on the slope during MS-5. These observations mark an important change in the behaviour of sediment gravity flows above MS-4 (discussed in more detail later).

Where preserved, MS-5 strata show clear thinning above the flanks of piercing salt diapirs shown on figure 24 (e.g. central parts of profiles S1 and S2; Fig. 12a), and commonly thin above the crests of lower slope folds that inverted MS-4 strata (above the toe of the BSW). Some canyons also appear to divert around these toe-folds. These observations indicate that these structure were actively growing during MS-5.

Mega-sequence 6 (MS-6) *– Turonian to Late Eocene (duration ~ 60 Ma)*

Like MS-5, MS-6 is thickest above the shelf, with very thin equivalent strata on the slope (Fig. 27). The lower boundary of MS-6 corresponds to the K94 marker located near the base of the chalky Petrel Member. Its upper boundary is a merger between shelf markers that define the top of the Eocene succession and a slope marker that corresponds to the top Eocene T35 marker described by Deptuck and Campbell (2012). MS-6 therefore includes the upper part of the Dawson Canyon Formation, Wyandot Formation, and the lowermost part of the Banquereau Formation (Wade and MacLean, 1990; Fig. 4).

The thickest parts of MS-6 generally correspond to Paleocene deltas perched on the shelf. They are offset landward and to the east relative to the thickest parts of MS-5. Seismic reflections on the shelf consist of low-angle prograding clinoforms that alternate with higher amplitude continuous but commonly faulted seismic reflections. The latter correspond to pelagic chalks of the Petrel Member, Wyandot Formation, Acadia chalk, or other unnamed Paleocene chalks (Wade and MacLean, 1990; Fensome et al., 2008). Well data indicates that the topset of shelf clinoform packages are sandy, with well-developed up-ward coarsening log motifs (e.g. Sachem, D-76). Foresets are generally muddy.
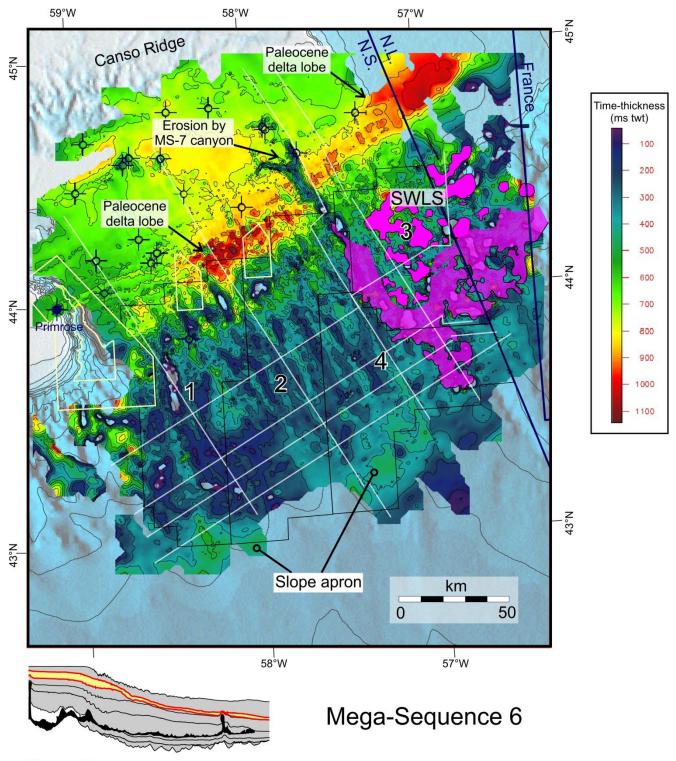
Mega-Sequence 6

Figure 27. Gridded time-thickness map of Mega-sequence 6 (Turonian through Eocene), representing about 60 Ma of time. The slope was largely sediment starved with periods of slope bypass. The outermost shelf and upper slope was very unstable during this period of time, with numerous slumps. Minor slope aprons formed in distal areas. Strata stored on the shelf are a combination of pelagic chalks and Paleocene to Eocene shelf-perched delta lobes.
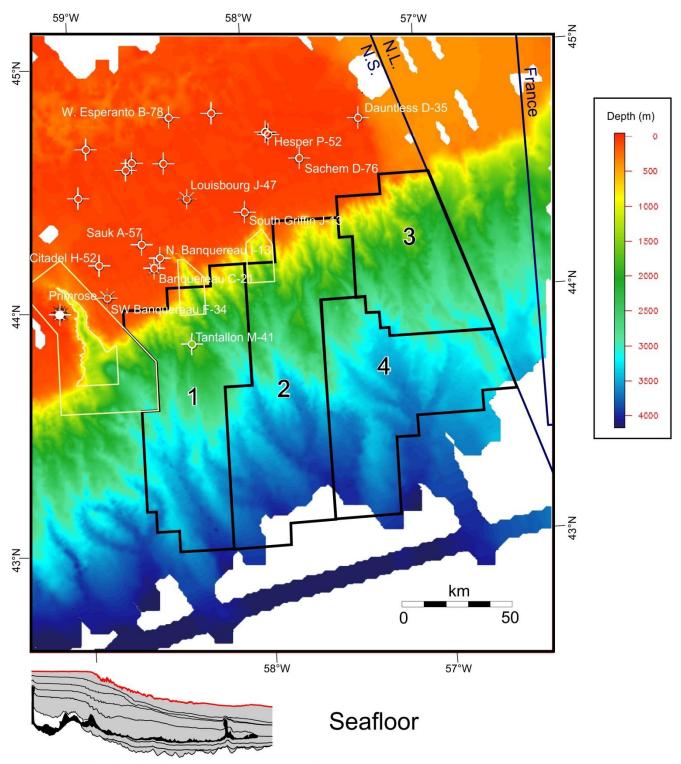
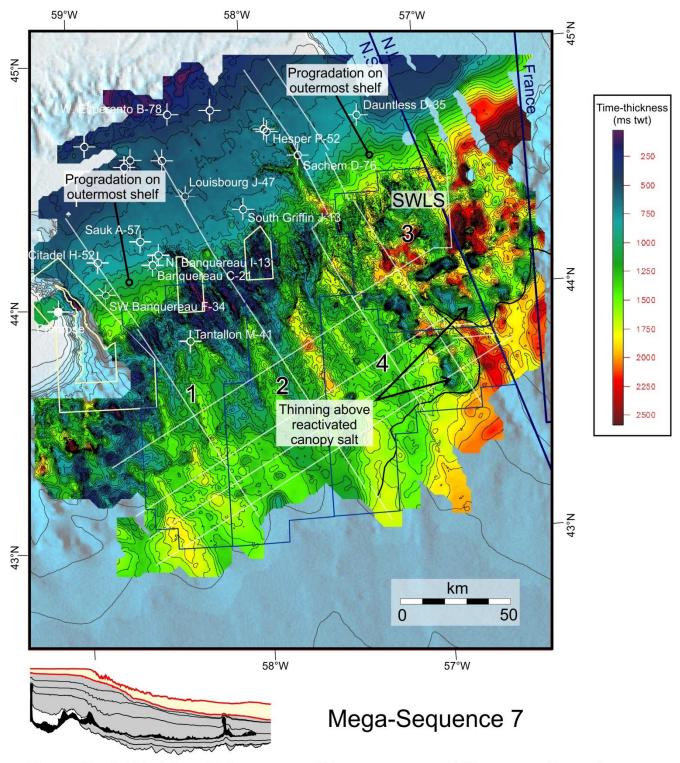**Figure 28.** Gridded depth map of the modern seafloor.

Figure 29. Gridded time-thickness map of Mega-sequence 7 (Oligocene to Recent).

MS-6 thins across the outer shelf towards the shelf edge established during MS-5. Numerous northeast-trending normal faults offset MS-6 here (Fig. 26). Further seaward, slope deposits are thin but highly complex, containing numerous unconformities and abundant evidence for slope failures and shallow detachment faults that sole out in the lower parts of MS-6 or the upper parts of MS-5. These are particularly common immediately seaward of shelf-edge trajectory 6 (Fig. 26) defining the seaward limit of MS-5 progradation. Wade et al. (1995) showed that numerous unconformities are present in this interval on the eastern Scotian Shelf, and several of them merge and are indistinguishable on the slope. Significant erosion is recorded across the MS-5 and MS-6 boundary, and it was not until the Middle Eocene that any appreciable amounts of strata finally accumulated above the K94 marker on the slope. These deposits strongly resemble time-equivalent Unit 1 of Campbell (2011) and sub-units 1a, 1b, and 1c of Deptuck and Campbell (2012) on the western Scotian margin, which record multiple periods of slope failure. The reader is directed to these sources for a more detailed account of these deposits.

Mega-sequence 7 (MS-7) – *post-Eocene (duration ~34 Ma)*

For the time being the remainder of the Cenozoic is grouped into MS-7 – a highly complex interval on the slope that is not yet fully understood. The lower boundary of MS-7 is the top Eocene T35 marker described above. Its upper boundary is the modern seafloor (Fig. 28), a heavily canyoned surface that strongly influences the thickness map in figure 29. In general, MS-7 is thickest to the northeast where it is more than 2.5 seconds thick (twt). It also shows a general increase in thickness down the slope. On the shelf, MS-7 consists of prograding clinoforms with prominent internal erosive surfaces. Prominent Oligocene and Miocene unconformities in the lower part of MS-7 on the shelf heavily erode underlying MS-6 strata. Some canyons can be traced for more than 50 km landward of the modern shelf edge (Fig. 29).

On the slope, small scale faults, sediment waves, and contourite drifts are common, as are mass transport deposits. Two 10-12 m thick unconsolidated Miocene sands were encountered at Tantallon M-41 on the upper slope. These probable turbidite sands range from fine to coarse grained and are moderately well sorted (see Kidston et al. 2007). The amalgamated salt canopy in the SWLS was reactivated during the early pats of MS-7. In some places more than 2 seconds (twt) of down-building took place within young minibasins on the slope. Pre-existing diapirs were squeezed in the early parts of MS-7, folding MS-6 strata that draped previously inactive salt bodies. MS-7 also thins above salt that was expelled from the SWLS. This reflects a combination of stratigraphic thinning above inflated salt sheets, but also poorly understood erosion along cryptic Oligocene or Miocene unconformities (e.g. seaward end of profile D4; Fig. 11). The substantial thickening of MS-7 in the southeastern study area reflects prominent onlap of alternating blocky mass transport deposits and wavy to continuous contourite drift-like deposits in the younger part of MS-7 (e.g. seaward ends of profiles D2, D3, and D4; Figs. 10, 11). These later deposits may be related to the onset of the Laurentian Fan.

Discussion – structural and stratigraphic evolution of the eastern Scotian slope

Mega-sequences 1 through 7 track important broad-scale sedimentary and/or structural changes on the eastern Scotian Slope. Ties to equivalent shelf successions, coupled with the use of salt contact maps, reconstruction of shelf-edge trajectories, and mapping of sediment thickness and structural trends, provide important insights into the structural and stratigraphic evolution of the eastern Scotian margin.

Basement rocks below the eastern Scotian Slope, whatever their origin, were flanked by two primary salt basins: the Huron Subbasin to the northwest (below the present-day outer shelf) and the SWLS to the northeast (below the present day slope). The narrow and elongated Huron Subbasin is a large graben that is

reasonably well constrained on seismic profiles. It is floored by faulted synrift clastics that gave way vertically to salt (see profiles D1 to D4; Figs. 10, 11), and is flanked in the seaward direction by the SGR, a probable horst block. Based on its landward position relative to the ECMA, the SGR is probably comprised of continental crust. The SWLS in contrast is poorly constrained on seismic profiles. The base salt and top basement surfaces appear to step deeper towards the SWLS (on time-structure maps; e.g. Fig. 30), but seismic imaging of the crust below this basin is very poor (e.g. profile S4 in Fig. 12b). As such, the placement of the original western and southern margins of the salt basin is highly speculative (Figs. 16, 30). The dextral (right-lateral) offset between these two salt basins presumably took place during rifting, across a relatively important transform fault zone, but this cannot be confirmed with existing data.

Because the age and origin of basement rocks to the southeast and southwest of the Huron Subbasin and SWLS, respectively, is uncertain, so too is the age of MS-1. If the highly rugose faulted basement rocks correspond to thin slow spreading oceanic crust above partially serpentinized mantle (our preferred interpretation, and consistent with Louden et al., 2012), then the interval immediately above it is probably equivalent to the earliest postrift sediments on the Scotian margin. In this scenario, MS-1 could be a distal equivalent of the Mohican Formation (Fig. 4) that accumulated passively in the Early to early Middle Jurassic in an area far removed from early river systems that continued to erode the rift shoulder at this time. Onlap of these deposits filled and smoothed over the steep rugged terrane produced by the early oceanic (or transitional) crust. Overall, MS-1 thins in both the seaward direction beneath to Sohm Abyssal Plain and in the landward direction towards the SGR, indicating that at a more regional scale MS-1 was deposited within a sag located between more elevated basement elements in both the landward and seaward directions. The 1.0 to 1.6 km high peaks produced by some rotated fault

blocks near the centre of this sag were largely filled in by the J175 marker at the top of MS-1.

MS-2 records the first pulse of more active sedimentation on the eastern Scotian Slope. Based on their distribution, MS-2 sediments appear to have been sourced from the northeast. Like MS-1, their age is uncertain, but the Bandol No. 1 well located 140 km to the northeast penetrated a several hundred meter thick intervals of Middle Jurassic (Bathonian to Callovian) sandstone, indicating that an active sediment delivery system was present in the Laurentian Subbasin prior to the Callovian. An early pulse of coarse sediment from this direction, towards the SWLS, is consistent with the thickness distribution of MS-2. MS-2 strata accumulated in front of salt that had begun to inflate and flow out of the SWLS, implying that the more proximal salt basin was also actively loaded at this time. At the same time, salt contacts indicate that salt flowed at least 45 km out of the Huron Subbasin and across the SGR (Ings and Shimeld, 2006), probably mostly during the latter parts of MS-2. Expulsion of this salt was triggered by Middle Jurassic sediment loading coupled with margin tilting in response to thermal subsidence (Shimeld, 2004; Ings and Shimeld, 2006; Albertz et al. 2010). As such, by the end of MS-2, two salt fronts were impinging on the eastern Scotian Slope from two directions (Fig. 16).

A westward shift in sediment delivery is recorded by well-developed progradation above the J163 marker along the northern margin of the Huron Subbasin in the early stages of MS-3 (Figs. 16, 21). Down-building in the Huron Subbasin was contemporaneous with the growth of the BSW. Mixed clastics and carbonates of the Mic Mac Formation were initially focused along the axis of the Huron Subbasin, and the wide spacing between early salt contacts seaward of the SGR implies that salt flowed rapidly down the slope relative to sediment aggradation in the early part of MS-3 (Fig. 16). Early slope sedimentation above the expelled salt was in the form of minibasins and roho systems. Some minibasins inverted to form turtles or half-turtles, as the early basins touched down onto a salt weld.
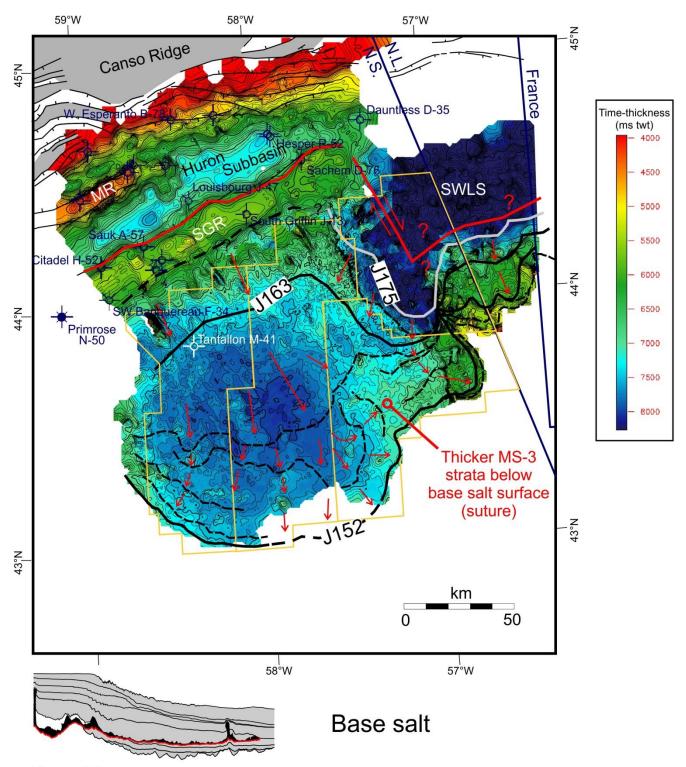
Figure 30. Gridded time-structure map along the base of the allochthonous salt layer on the slope, correlated landward along the base of the autochthonous salt layer in the Huron Subbasin, and merged with the tentatively picked top basement surface below the southwest Laurentian Subbasin (SWLS). Red bold lines approximate the seaward edges of the primary salt basins. In the SWLS this line is highly schematic. Salt contacts and interpreted expulsion vectors are also shown. Synrift dextral strike-slip is inferred based on offset between salt basins.

Contemporaneous seaward translation of the BSW above the salt detachment, however, transported many of the early turtles seaward, where they are clustered along marginal areas of the BSW (Fig. 31). Subtle contractional features formed locally at the same time, but most extension was accommodated down slope through the narrowing of salt bodies or along the open, seaward end of the system (Ings and Shimeld, 2006).

The pattern of sediment thickness preserved *below* the central and western parts of the salt detachment, used together with salt contact maps, implies that salt advanced somewhat unevenly down the slope as two or three separate tongues, with the eastern salt tongue advancing towards the southeast ahead of the others (Fig. 16). At the same time, salt continued to flow, at a slower rate, out of the SWLS and away from the J163 salt contact. A ridge of thicker sub-salt strata is preserved along the boundary between these advancing salt fronts, where sediment accumulated along an open corridor that remained uncovered by salt for a longer period of time (relative to immediately adjacent areas). This ridge separates the central and western parts of the BSW from its eastern part. A final salt suture probably formed somewhere above this sediment ridge as the two salt fronts converged prior to the extinction of the BSW. As such, detachment along the base of the BSW appears to have taken place above salt from both subbasins. The J150 salt contact along the seaward boundary of the BSW still shows an indentation where salt from these two subbasins merged (Fig. 16).

The latest Jurassic Avalon Uplift at the onset of MS-4 coincides with a change in shelf lithofacies, where the mixed clastics and carbonates of the Mic Mac Formation were replaced by coarse siliciclastics of the Missisauga Formation (Wade and MacLean, 1990). The initiation of the Avalon Uplift is regarded as latest Kimmeridgian or early Tithonian in the Jeanne d'Arc Basin (Grand Banks of Newfoundland), with rejuvenated periods of uplift continuing into the Barremian (McAlpine, 1990). Uplift has been attributed to renewed rifting between the Grand Banks and Iberia, and sedimentation rates into the Jeanne d'Arc Basin reportedly doubled after uplift began, a time when some of the most important reservoirs were deposited (McAlpine, 1990). On the eastern Scotian shelf, uplift is recorded by the abrupt thinning and onlap of MS-4 strata above the J152 marker in the northern study area, along the southwestern flank of the Avalon Uplift (Figs. 6, 22). MS-4 records a noticeable westward shift away from the Avalon Uplift, and marks the end of down-building into the Huron Subbasin, with sedimentation instead focused seaward of the SGR (Fig. 22).

On the eastern Scotian slope, the onset of Avalon Uplift marks the termination of the BSW and the onset of the Missisauga fan complex. The exact relationship between the Avalon Uplift and the transitional interval on the slope between the J152 marker and the prominent unconformity near the base of MS-4 is unclear (dark grey interval in Figs. 10-12). The interval may record a complex period of slope regrading in response to a change in the gradient profile triggered during the initial onset of the Avalon Uplift. The unconformity above the dark grey interval may have formed during a period of rejuvenated uplift on the eastern Scotian Shelf, sometime after the initial onset of the Avalon Uplift. In this latter scenario, the unconformity probably corresponds to the near-base Cretaceous Unconformity described on the shelf between Berriasian and Valanginian strata (corresponding to the K137 marker of OETR, 2011; see also Weston et al., 2012). In either case, the succession above this important slope unconformity marks the widespread aggradation of submarine fans above the BSW. Increased accumulation of submarine fans seaward of the BSW, particularly in the southwestern study area, appears to have buttressed the salt-based detachment. This halted much of the seaward translation of the BSW, and any subsequent upslope extension was instead accommodated downslope by the contraction of pre-existing salt bodies remaining within or at the seaward termination of the BSW (Fig. 21; see also Ings and Shimeld, 2006).

The abrupt seaward shift in MS-5 shelf-edge clinoforms in the Albian and Cenomanian, despite the overall aggradational character of shelf strata at this time, is a testament to the continued ample supply of clastic sediments to the margin after late Aptian flooding (although on average with a lower net-to-gross than the underlying Missisauga Formation). At no other time before or since, going back as far as the break-up between Morocco and Nova Scotia, has the continental shelf edge been located further seaward than it was during this period. Even the modern continental shelf edge is located at least 20 km landward of this Albian-Cenomanian maximum regression, which today sits beneath more than 1500 m of water. Significantly more sediment was stored on the shelf however, than on the slope during MS-5.

The abrupt Early Albian seaward shift in the shelf edge coincides with a marked change in submarine fan architecture on the slope. The MS-5 slope is dominated by empty canyons flanked by wedge-shaped inter-canyon highs or levees of the Shortland fan complex. This implies that the lack of sediment storage on the slope during MS-5 (compared, for example, to MS-4) is the result of erosion and sediment bypass of at least the coarse fraction of flows across the slope, rather than sediment starvation. Only the finer grained upper parts of turbiditiy currents that overspilled canyon margins appear to have accumulated to any significant degree on the slope. Coarser-grained submarine fan deposits must have accumulated somewhere seaward of these canyons, beyond the limits of our study area.

Although growth across outer shelf listric faults is recorded within MS-4, it was not until MS-5 that growth faults on the upper slope were balanced by shortening on the lower slope. MS-5 is the first interval to show clear thinning above the salt-cored folds that inverted MS-4 turbidites above the seaward parts of the BSW (Fig. 25). The abrupt change from aggradational channel-levee systems in the Missisauga fan complex to bypassing canyons flanked by levees in the Shortland fan system, coupled with the timing of the onset of folding of MS-4 strata above the toe of the BSW, might

indicate that the slope began to steepen during deposition of MS-5. This would explain the change in submarine fan architecture and perhaps why, despite the clear growth across listric faults during MS-4 immediately upslope from the BSW, there is no evidence of the onset of folding of MS-4 strata until MS-5. We are not sure what would cause the slope to steepen, but a late Aptian to early Albian volcanic center has been described near the Orpheus Graben northwest of the study area (Bowman et al., 2012). Volcanism here coincides with the onset of MS-5 so perhaps there is an indirect relationship between this event and the abrupt change in fan architecture in the study area.

Preferential storage of sediments on the shelf continued during MS-6, when a period of generally high sea level and reduced sediment supply pushed rivers far back from the MS-5 continental shelf edge. Numerous regressions in the latest Cretaceous, Paleocene, and Eocene produced local build-outs of delta lobes with sandy topsets and muddy clinoforms, but these did not advance beyond the outer shelf. More time is recoded in MS-6 (~60 Ma) than any other mega-sequence described in this report, yet only a thin succession accumulated on the slope over a time span that lasted three times longer than MS-5. Accumulation of weak, water-saturated chalks appear to have pre-conditioned the slope for failure, and numerous slumps, periods of slope detachments, and merged unconformities are all recorded within this thin slope succession. In contrast to MS-5, the lack of sediment stored on the slope during MS-6 probably reflects a combination of sediment starvation and slope bypass. The outer shelf subsided during MS-6, and the nucleation of slope failures and shallow detachment faults immediately above the MS-5 shelf edge (the maximum regression of the margin) could reflect a broader scale attempt by MS-6, followed by MS-7 depositional systems, to regrade the slope. The ~51 Ma Montagnais marine bolide impact on the outer shelf ~450 km southwest of the study area took place about mid-way through MS-6 (Jansa et al., 1989; Deptuck and Campbell, 2012). This important event

45

may have contributed to the apparent slope instability at this time, but numerous additional older and younger slumps and erosional surfaces indicate the margin was failure prone even without this celestial impact event.

Finally, MS-7 records a sharp change back to slope-dominated sedimentation, with thick outer shelf and slope deposits comprised of turbidites, contourite drifts, and widespread mass transport deposits. The Laurentian Fan was deposited during this interval, and periods of shelf-crossing glaciation strongly affected slope sedimentation (see Piper et al., 2012).

Exploration potential

Potential reservoirs

MS-3 and MS-4 are considered the most important reservoir intervals in the NS14-1 Call area. There is no direct well calibration for MS-3 on the slope, but shelf wells indicate the sediment delivery systems were a complex mixture of clastics and carbonates corresponding to the Mic Mac Formation. Carbonates may have preferentially accumulated on the outer shelf during periods of high sea level with clastics preferentially delivery into deepwater during periods of falling and low sea level. The strong, continuous reflections within complex structures of the BSW in Parcels 1, 2, and 4 may correspond to impedance contrasts between carbonates and turbidite sands. It is also possible that some of the more continuous and commonly folded reflections within the BSW correspond to calci-clastic submarine fans shed from the mixed clastic-carbonate system located above the SGR. Secondary porosity development could make these favourable reservoirs. Calcite cementation and poor porosity preservation due to burial depth are key risk factors for potential reservoirs in MS-3.

MS-4 is considered the most important reservoir interval, supplied by fluvial deltaic sands of the Missisauga Formation. Seismic facies in Parcels 1, 2, and 4 are consistent with the aggradation and migration of turbidite channels flanked by levees. We anticipate

some lateral confinement of turbidite corridors on the upper slope, with reservoirs consisting primarily of amalgamated channels. Note that Tantallon M-41 likely missed the turbidite corridor in this proximal setting (Piper et al., 2010). We anticipate a progressive downslope decrease in confinement of turbidite corridors owing to avulsion of channel systems and deposition of unconfined sheet sands in submarine lobe or frontal splay settings. This trend has been documented in many modern analogues (e.g. Piper and Normark 2001; Deptuck et al., 2008), and is supported by direct observation from seismic profiles in the study area (Fig. 23). Because of the seaward shift in the shelf edge position from the base of MS-4 to the top, deeper intervals will be located further from the shelf edge. As such, there is increase potential for encountering less confined, more distal turbidite settings in the deeper parts of MS-4. There are also indications that subtle morphological variations were present on the slope in Parcels 1, 2, and 4 during deposition of the Missisauga fan complex. Future efforts should focus on identifying potential paleo-steps on the upper slope that may have led to more widespread sheet-like turbidite reservoirs in an upper slope position (see Deptuck et al., 2012 and references therein). 3D seismic volumes are required for such efforts.

Finally, turbidites of the Missisauga fan complex were probably also deposited in the SWLS. Trapping of sands on this part of the slope was probably quite efficient owing to the increased complexity of the slope morphology and corresponding increased potential for ponding of turbidites. Improved seismic imaging in this very complex salt tectonic setting is needed to better define turbidite corridors through the SWLS. Modern seismic data may also help discriminate between high and low porosity sands as well as gas charged sands. For example, Goodway et al. (2008) described the results of an Amplitude Variation with Offset (AVO) and Lambda-Mu-Rho (LMR) analysis conducted over the Stonehouse exploration license held by Encana from Jan, 1, 2002 to Dec. 31, 2007. AVO analysis can be used to detect anomalies due to highly porous hydrocarbon
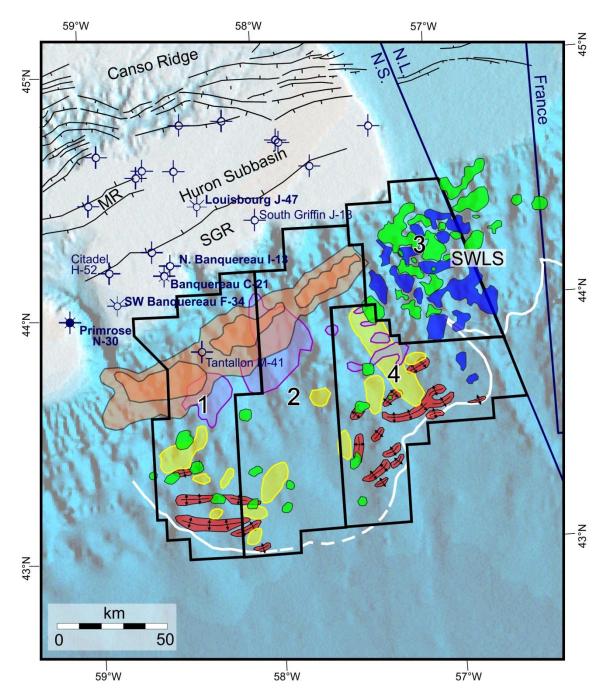
Figure 31. Distribution of different structural styles in the NS14-1 Call for Bids area. Orange areas correspond to potential rollover structures associated with reactivation of upper slope listric faults. Potential turbidite-bearing strata of MS-4 were inverted into large folds here. Similarly, **Red** areas correspond to symmetrical folds initiated during MS-5 extension that was balanced down slope by inversion of MS-4 turbidites. Yellow areas correspond to potential Jurassic turtles or half-turtles within the BSW, and **Purple** areas show potential Jurassic contractional structures within the BSW. **Green** shows the distribution of shallow salt structures, and **Blue** shows the located of Cretaceous to Tertiary minibasins in the southwest Laurentian Subbasin (SWLS).

filled reservoirs, while LMR inversion can provide information about the rock properties of potential reservoirs. Modeled data based on the Annapolis G-24 and Tantallon M-41 wells predicts that high porosity gas sands thicker than 10 m will produce bright AVO responses that are clearly distinguishable from high porosity wet sands or low porosity wet or gas sands (Goodway et al., 2008). The study also points to asignificant number of positive Upper Missisauga AVO anomalies within the northern portion of Parcel 2.

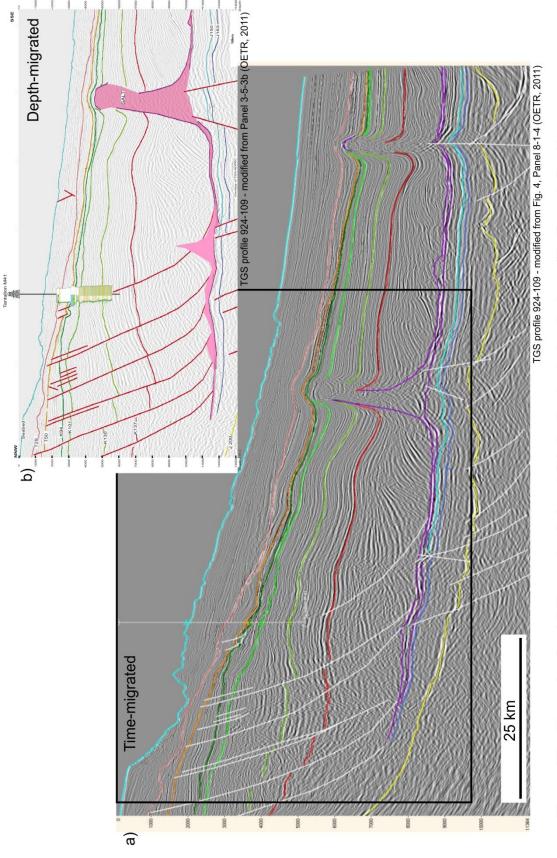### Potential hydrocarbon-bearing structures

Each of the NS14-1 parcels contains a range of potential Cretaceous and Jurassic drilling targets. Figure 31 summarizes the distribution of potential traps and minibasins. Parcels 1 and 2 cover the proximal to distal reaches the BSW, which contains a range of potential hydrocarbon-bearing structures that developed during a complex period of salt tectonics. Numerous turtles and half turtles are recognized in Parcels 1, 2, and 4. Local shortening also appears to have produced several folds and local thrust sheets in the headward parts of the BSW. Overthrusting of over-rotated basins in roho systems also generated potential traps in the BSW.
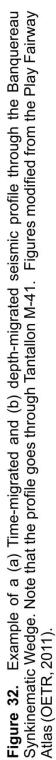
Reactivation of the Middle to latest Jurassic BSW in the mid-Cretaceous to Eocene inverted a Lower Cretaceous succession strongly believed to contain sandy turbidites (Missisauga fan complex). Several salt-cored buckle folds containing MS-4 strata are present on the lower slope, particularly in the seaward parts of Parcels 1 and 4 (Figs. 31). Deep water depths here may prohibit testing some of these structures. The most promising drilling targets correspond to a series of large, long-wavelength folds found on the upper to middle slope above the headward parts of the BSW in Parcels 1 and 2. These folds, termed the "stonehouse trend", are 15 to 20 km wide and 20 to 40 km long, with potential four-way dip closure areas in excess of 200 km^2 (based on regional depth structure map presented on Panel 5-3-8b of OETR, 2011). Tantallon M-41, which encountered a ~10 m interval of gas charged sands in the lower parts of the Missisauga fan complex (Goodway et al., 2008), is located along the stonehouse

trend, but appears to have been positioned in a saddle region between two large rollover structures on the K130 depth structure map (OETR, 2011). Amplitude extractions from a modern 3D seismic volume along strike from Tantallon M-41 (from the Stonehouse 3D survey) reveal a number of geobodies that likely correspond to porous sands associated with amalgamated turbidite channels (Goodway et al., 2008). Such data were not available when the Tantallon well was drilled in 1986. A comparison of time-migrated and depth-migrated seismic profiles illustrates the importance of modern depth data for defining structural closure along this trend (e.g. Fig. 32). Likewise, modern processing is needed to better define potential turbidite reservoirs within these structures. The timing of folds along the stonehouse trend is ideal because it immediately post-dates the period of widespread turbidite deposition on the slope associated with the Missisauga fan complex.
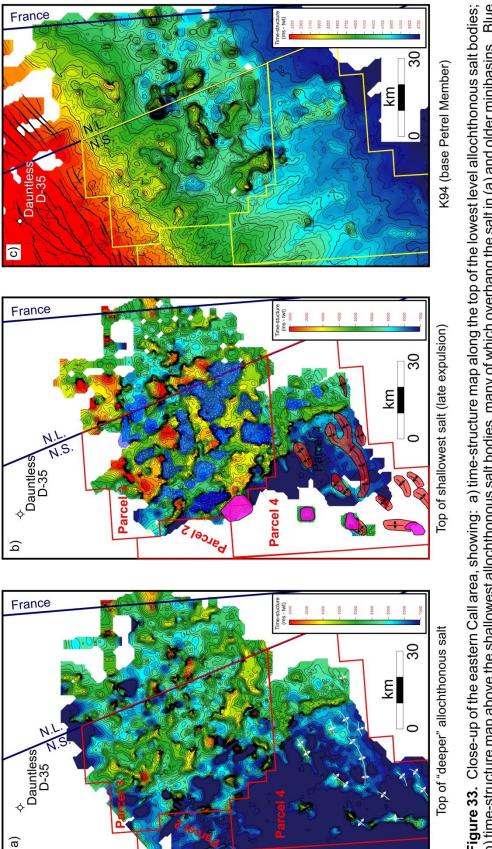
Parcel 3 is located above southwest Laurentian Subbasin (SWLS). Salt-related structures in Parcel 3 are complex, with as many as three tiers of allochthonous salt that create a wide variety of potential trap configurations, but also substantially degrade seismic imaging. The seaward half of Parcel 3 is located above the Southwest Laurentian Salt Canopy that was expelled from the SWLS. Time-structure maps above the deepest allochthonous salt surface provide an indication of the distribution of minibasins, parts of which were covered by one or more shallower tiers of more recently expelled salt (compare Figs. 33a and 33b). Numerous potential minibasin, salt flank, and sub-salt targets exist in Parcel 3. Further seaward, Parcel 4 is located in a complex region of loading and detachment above salt that was expelled from both the BSW and the SWLS. Structures include potential turtles and salt-cored folds, but the deep water depths here will pose additional exploration challenges.

Source rocks

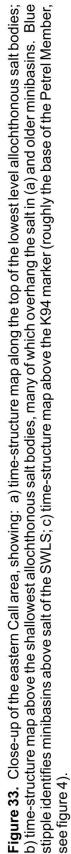Both gas and oil prone source rocks are possible for the NS14-1 Call area. Oil and gas discoveries have been made on the outer shelf just landward of the Call area

Figure 32. Example of a (a) Time-migrated and (b) depth-migrated seismic profile through the Banquereau Synkinematic Wedge. Note that the profile goes through Tantallon M-41. Figures modified from the Play Fairway Atlas (OETR, 2011).

Figure 33. Close-up of the eastern Call area, showing: a) time-structure map along the top of the lowest level allochthonous salt bodies; b) time-structure map above the shallowest allochthonous salt bodies, many of which overhang the salt in (a) and older minibasins. Blue stipple identifies minibasins above salt of the SWLS; c) time-structure map above the K94 marker (roughly the base of the Petrel Member, see figure 4).

(e.g. oil and gas in Primrose N-50, gas in Banquereau C-21), with several additional wells encountering flow tested gas shows (e.g. N. Banquereau I-13, SW Banquereau F-34, Louisbourg J-47), minor gas shows (Citadel H-52, South Griffin J-13, Tantallon M-41), or spotted oil staining (e.g. South Griffin J-13) (Fig.31). In addition, up to 5% TOC type II to III source rocks were encountered in Tithonian strata in Louisbourg J-47 (OETR, 2011), less than 40 km northeast of Parcels 1 and 2. A review of this and other potential source rocks is provided in the following section. It should be noted, however, that our choice to carry the top Jurassic marker above the Banquereau Synkinematic Wedge, rather than below it as was done in the Play Fairway Study, will substantially alter the source rock maturation work published in OETR (2011) for the eastern Scotian Slope, and for areas underlying the Sable Slope Canopy further west. For Middle to Late Jurassic source rocks, this change could have a positive impact (bringing them into the oil window at a later stage). For older source rocks below the Banquereau Synkinematic Wedge, like the theoretical Pleinsbachian (OETR, 2011) that is already overcooked in the NS14-1 Call area, this change means these source rocks would have been buried deeper for a longer period of time.

Recommended citation
Deptuck, M.E., Kendell, K., Brown, D.E., Smith, B. (2014), Seismic stratigraphic framework and structural evolution of the eastern Scotian Slope: geological context for the NS14-1 Call for Bids area, offshore Nova Scotia, CNSOPB Geoscience Open File Report 2014-001MF, 58 p.

References

Albertz, M., Beaumont, C., Shimeld, J., Ings, S.J., and Gradmann, S. (2010) An investigation of salt tectonics strutural styles in the Scotian Basin, offshore Atlantic Canada: 1. Comparison of observations with geometrically simple numerical models, Tectonics, v.29, doi:10.1029/2009TC002539

Bowman, S.J., Pe-Piper, G., Piper, D.J.W., Fensome, R.A. and King, E.L. (2012) Early Cretaceous volcanism in the Scotian Basin, Canadian Journal of Earth Sciences, v. 49, p. 1523-1539

Campbell, D.C. (2011) The Late Cretaceous and Cenozoic geological history of the outer continental margin off Nova Scotia, Canada: Insights into margin evolution from a mature passive margin, PhD Dissertation, Department of Earth Sciences, Dalhousie University, Halifax, Nova Scotia.

Campbell, D.C. and Deptuck, M.E. (2012) Alternating bottom current dominated and gravity flow dominated deposition in a lower slope and rise setting – insights from the seismic geomorphology of the western Scotian margin, Eastern Canada, In: B. Prather, M. Deptuck, D. Mohrig, B. van Hoorn, and R. Wynn (Eds), Application of the Principles of Seismic Geomorphology to Continental Slope and Base-of-slope Systems: Case Studies from Seafloor and Near-Seafloor Analogues, SEPM Special Publication 99, p. 329-346

CNSOPB (2013) Geological context and parcel prospectivity for Call for Bids NS13-1: Seismic interpretation, source rocks and maturation, exploration history and potential play types of the central and eastern Scotian Shelf, Canada-Nova Scotia Offshore Petroleum Board Call for Bids NS13-1, 66p. www.callforbids.ca/sites/default/files/inline-pdf/cfb_ns13_summary-final_for_web_2.pdf

Dehler, S.A. (2012) Initial rifting and breakup between Nova Scotia and Morocco: insight from new magnetic models, Canadian Journal of Earth Sciences, v. 49, p. 1395-1415

Dehler, S.A. (2010) Initial rifting and break-up between Nova Scotia and Morocco: An examination of new geophysical data and models, in Conjugate Margins II, Lisbon 2010, Metedo Directo, v. VIII, p. 79-82, ISBN: 978-989-96923-1-2, http://metedodirecto.pt/CM2010

Deptuck, M.E. (2011) Proximal to distal postrift structural provinces on the western Scotian Margin, offshore Eastern Canada: Geological context and parcel prospectivity for Call-for-Bids NS11-1, Canada-Nova Scotia Offshore Petroleum Board, Geoscience Open File Report (GOFR) 2011-001MF, 42p. www.cnsopb.ns.ca/sites/default/files/pdfs/gofr__2011_001mf.pdf

Deptuck, M.E. and Campbell, D.C. (2012) Widespread erosion and mass failure from the ~51 Ma Montagnais marine bolide impact off southwestern Nova Scotia, Canada, Canadian Journal of Earth Sciences, v. 49, p. 1567-1594

Deptuck, M.E., Steffens, G.S., Barton, M., Pirmez, C. (2003) Architecture and evolution of upper fan channel-belts on the Niger Delta slope and in the Arabian Sea, Marine and Petroleum Geology, v. 20, p. 649-676

Deptuck, M.E., Sylvester, Z., Pirmez, C., O'Byrne, C. (2007) Migration-aggradation history and 3-D seismic geomorphology of submarine channels in the Pleistocene Benin-major Canyon, western Niger Delta slope, Marine and Petroleum Geology, v.24, p. 406-433

Deptuck, M.E., Piper, D.J.W., Savoye, B., and Gervais, A. (2008) Dimensions and architecture of late Pleistocene submarine lobes of the northern margin of East Corsica, Sedimentology, v. 55, p. 869-898

Deptuck, M. E., Sylvester, Z., and O'Byrne, C. (2012) Pleistocene seascape evolution above a 'simple' stepped slope, western Niger Delta, In: B. Prather, M.E. Deptuck, D. Mohrig, B. van Hoorn, and R. Wynn (Eds), Application of the Principles of Seismic Geomorphology to Continental Slope and Base-of-slope Systems: Case Studies from Seafloor and Near-Seafloor Analogues, SEPM Special Publication 99, p. 199-222

Ebinger C.A. and Tucholke, B.E. (1988) Marine Geology of the Sohm Basin, Canadian Atlantic Margin, AAPG Bulletin, v. 72, p. 1450-1468

Fensome, R.A., Crux, J.A., Gard, I.G., MacRae, R.A., Williams, G., Thomas, F., Fiorini, F., and Wach, G. (2008) The last 100 million years on the Scotian Margin, offshore eastern Canada: An event-stratigraphic scheme emphasizing biostratigraphic data, Atlantic Geology, v. 44, p. 93–126

Fletcher, R.C., Hudec, M.R., and Watson, I.A. (1995) Salt glacier and composite sediment-salt glacier models for the emplacement and early burial of allochthonous salt sheets, In: M.P.A. Jackson, D.G. Roberts and S. Snelson (Eds), Salt Tectonics: a global perspective. AAPG Memoir 65, p. 77-108

Funck, T., Jackson, H.R., Louden, K., Dehler, S.A. and Wu, Y. (2004), Crustal structure of the northern Nova Scotia rifted continental margin (Eastern Canada), Journal of Geophysical Research, v. 109, B09102

Goodway, B., Szelewski, C., Overell, S., Corbett, N. and Skrypnek, T (2008). Calibrated AVO and LMR analysis using a new DHI flat-spot AVO class 6 fluid contact to mitigate reservoir risk at Stonehouse, offshore Nova Scotia, Canadian

Society of Exploration Geophysicists Recorder, v. 22 (October, 2008), p. 23-32

Haworth, R.T., and Lefort, J.P. (1979) Geophysical evidence for the extent of the Avalon zone in Atlantic Canada, Canadian Journal of Earth Sciences, v. 16, p. 552-567

Ings, S.J., and Shimeld, J.W. (2006) A new conceptual model for the structural evolution of a regional salt detachment on the northeast Scotian margin, offshore eastern Canada, AAPG Bulletin, v. 90, p. 1407-1423

Jansa, L.F. and Wade, J.A. (1975) Geology of the continental margin off Nova Scotia and Newfoundland, In: W.J.M van der Linden and J.A. Wade (Eds), Offshore Geology of Eastern Canada, Geological Survey of Canada Paper 74–30, p. 51–105

Jansa, L.F., Pe-Piper, G., Robertson, P.B., and Friedenreich, O. (1989) Montagnais: A submarine impact structure on the Scotian Shelf, eastern Canada, Geological Society of America Bulletin, v. 101, p. 450-463

Jansa, L.F., Pe-Piper, G., and Loncarevic, B. (1993) Appalachian basement and its intrusion by Cretaceous dykes, offshore southeast Nova Scotia, Canada, Canadian Journal of Earth Sciences, v. 30, p. 2495-2509

Keen, C.E., and Beaumont, C. (1990) Geodynamics of rifted continental margins, Chapter 9, In: Geology of the Continental Margin of Eastern Canada, M.J. Keen & G.L. Williams, (Eds), Geological Survey of Canada, The Geology of Canada, p. 391-472

Keen, C.E., Loncarevic, B.D., Reid, I., Woodside, J., Haworth, R.T., and Williams, H. (1990) Tectonic and geophysical overview, Chapter 2, In: Geology of the Continental Margin of Eastern Canada, M.J. Keen & G.L. Williams, (Eds), Geological Survey of Canada, The Geology of Canada, p. 33-85

Keen, C.E., and Potter, D.P. (1995) The transition from a volcanic to nonvolcanic rifted margin off eastern Canada, Tectonics, v. 14, p. 359-371

Kidston, A.G., Smith, B.M., Brown, D.E., Makrides, C., and Altheim, B. (2007) Nova Scotia deepwater postdrill analysis, 1982-2004, Canada Nova Scotia Offshore Petroleum Board, Halifax, Nova Scotia, 181 p. www.cnsopb.ns.ca

Klitgord, K.D. and Schouten, H. (1986) Plate Kinematics of the central Atlantic, in Vogt, P.R. and Tucholke, B.E. (Eds), The Geology of North America, Volume M, The Western North Atlantic Region: Geological Society of America, p. 351-378

Labails, C., Olivet, J.-L., Aslanian, D., and Roest, W.R. (2010) An alternative early opening scenario for the Central Atlantic

Ocean, Earth and Planetary Scientific Letters, v. 297, p. 355-368

Lau, K.W.H., Louden, K.E., and Nedimovic, M. (2010) Variations in crustal structure across the Nova Scotia continental margin and its conjugate, In: R. Pena dos Ries and N. Pimentel (Eds), Rediscovering the Atlantic: New ideas from an old sea – Extended Abstracts. II Central and North Atlantic Conjugate Margins, Lisbon 2010, p. 142-146, ISBN: 978-989-96923-1-2

Louden, K., Wu, Y. and Tari, G.C. (2012) Systemic variations in basement morphology and rifting geometry along the Nova Scotia and Morocco conjugate margins, In: W.U. Mohriak, A. Danforth, P.J. Post, D.E. Brown, G.C. Tari, M. Nemčok, and S.T. Sinha, (Eds), Conjugate Divergent Margins. Geological Society of London, Special Publications 369, p. 267-287

MacLean, B.C. and Wade, J.A. (1992) Petroleum geology of the continental margin south of the islands of St. Pierre and Miquelon, Offshore Eastern Canada, Bulletin of Canadian Petroleum Geology, v. 40, p. 222-253

McAlpine, K.D. (1990) Mesozoic stratigraphy, sedimentary evolution and petroleum potential of the Jean d'Arc basin, Grand banks of Newfoundland, Geological Survey of Canada Paper 89-17, 50p.

Oakey, G.N. and Dehler, S.A. (2004) Atlantic Canada Magnetic Map Series: Atlantic Canada, Geological Survey of Canada, Open File 1813, 1:3000000

OETR (2011) Play Fairway Analysis Atlas - Offshore Nova Scotia, Nova Scotia Department of Energy Report, NSDOE Records Storage File No. 88-11-0004-01, 347p. http://www.offshoreenergyresearch.ca/OETR/OETRPlayFairwayProgramMainPage/tabid/402/Default.aspx

Pe-Piper, G. and Jansa, L.F. (1999) Pre-Mesozoic basement rocks offshore Nova Scotia, Canada: new constraints on the origin and Paleozoic accretionary history of the Meguma terrane, Bulletin of the Geological Society of America, v. 111, p. 1773-1791

Pe-Piper, G. and Piper, D.J.W. (2004) The effects of strike-slip motion along the Cobequid-Chedabucto-southwest Grand Banks fault system on the Cretaceous-Tertiary evolution of Atlantic Canada, Canadian Journal of Earth Sciences, v. 41, p. 799-808

Pe-Piper, G., Piper, D.J.W., Jansa, L.F., and de Jonge, A. (2007) Early Cretaceous opening of the North Atlantic Ocean: Implications of the petrology and tectonic setting of the Fogo Seamounts off the SW Grand Banks, Newfoundland, Geological Society of America Bulletin, v. 119, p. 712-724

Piper, D.J.W., and Deptuck, M. (1997) Fine-grain turbidites of the Amazon fan: facies characterization and interpretation, In: R.D. Flood, D.J.W. Piper, A. Klaus and L.C. Petersen (Eds), Proceedings of the Ocean Drilling Program - Scientific Results, v. 155, p. 109-146

Piper, D.J.W., and Normark, W.R. (2001) Sandy fans: From Amazon to Hueneme and beyond, AAPG Bulletin, v. 85, p. 1407-1438

Piper, D.J.W., Noftall, R. and Pe-Piper, G. (2010) Allochthonous prodeltaic sediment facies in the lower Cretaceous at the Tantallon M-41 well: Implications for the deep-water Scotian Basin, AAPG Bulletin, v. 94, p. 87-104

Piper, D.J.W., Deptuck, M.E., Mosher, D.C., Hughes-Clarke, J.E., and Migeon, S. (2012) Erosional and depositional features of glacial meltwater discharges on the eastern Canadian continental margin, In: B. Prather, M. Deptuck, D. Mohrig, B. van Hoorn, and R. Wynn (Eds), Application of the Principles of Seismic Geomorphology to Continental Slope and Base-of-slope Systems: Case Studies from Seafloor and Near-Seafloor Analogues: SEPM Special Publication 99, p. 61-80

Shimeld, J. (2004) A comparison of salt tectonic subprovinces beneath the Scotian Slope and Laurentian Fan, 24th Annual GCS-SEPM Foundation Bob F. Perkins Research Conference, Houston, p. 291-306

Sibuet, J.-C., Rouzo, S. and Shrivastava, S. (2012) Plate tectonic reconstructions and paleogeographic maps of the Central and North Atlantic oceans, Canadian Journal of Earth Sciences, v. 49, p. 1395-1415

Smith, B.M., Deptuck, M.E., and Kendell, K.L. (2010) Upper Cretaceous mass transport systems above the Wyandot Formation chalk, offshore Nova Scotia, In: D. Mosher et al. (Eds), Submarine Mass Movements and Their Consequences, Advances in Natural and Technological Hazards Research. Kluger-Springer Bookseries, v. 28, p. 605-616

Swift, S.A., Ebinger, C.J., and Tucholke, B.E. (1986) Seismic stratigraphic correlation across the New England Seamounts, western North Atlantic Ocean, Geology, v. 14, p. 346-349

Tankard, A.J., and Balkwill, H.R. (1989) Extension tectonics and stratigraphy of the North Atlantic Margins: Introduction, Chapter 1, In A.J. Tankard and H.R. Balkwill, (Eds) Extensional Tectonics and Stratigraphy of the North Atlantic Margins, AAPG Memoir 46, p. 1-6

Vogt, P.R. (1973) Early events in the opening of the North Atlantic, In: D.H. Tarling and S.K. Runcorn (Eds), Implications of Continental Drift to the Earth Sciences, NATO ASI Series, Academic Press, New York, p. 963-712

Wade, J.A. and MacLean, B.C. (1990) The geology of the Southeastern Margin of Canada, Chapter 5, In: M.J. Keen and G.L. Williams (Eds), Geology of the Continental Margin of Eastern Canada, Geological Survey of Canada, The Geology of Canada, p. 190-238
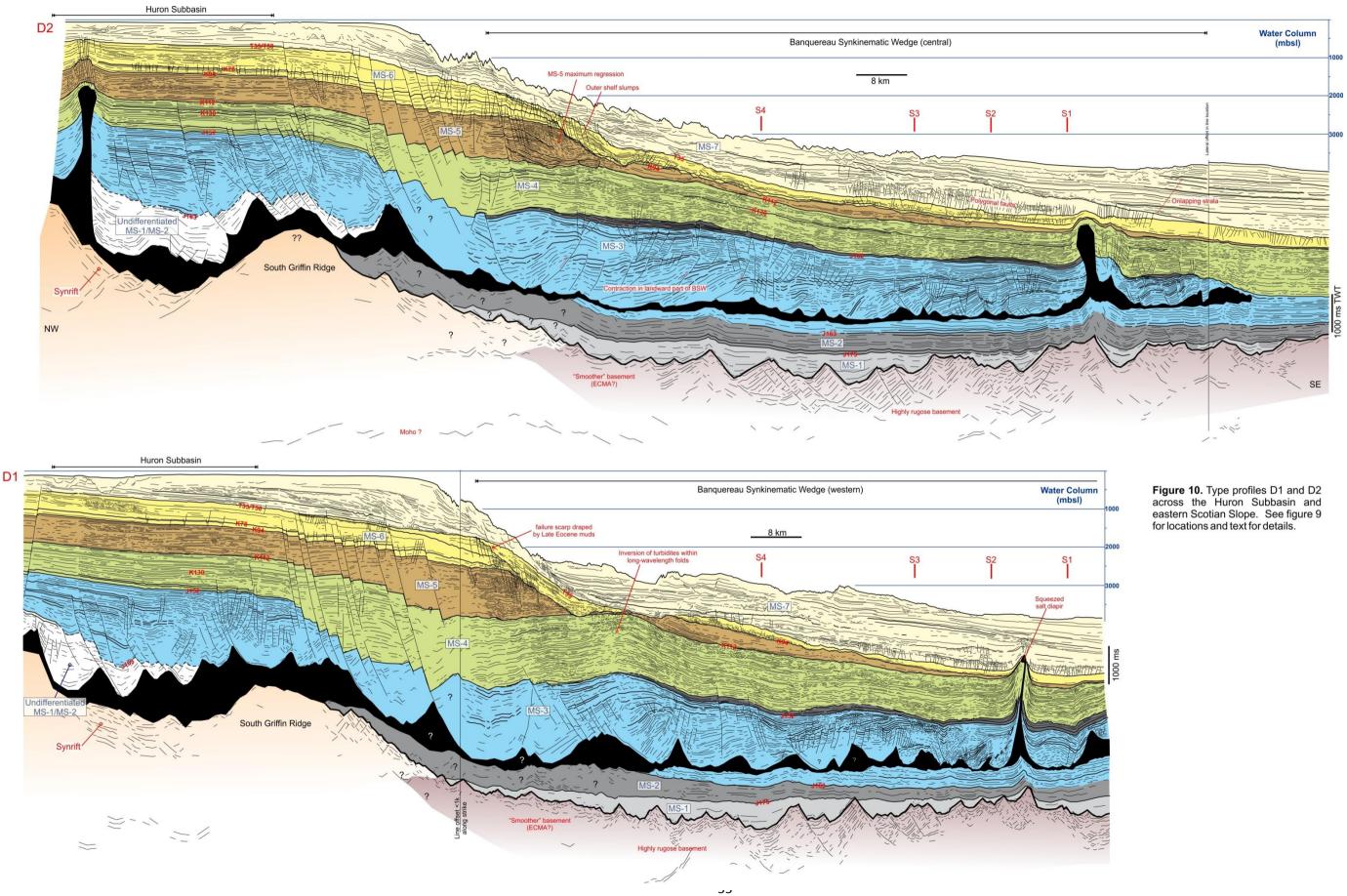
Wade, J.A., MacLean, B.C. and Williams, G.L. (1995) Mesozoic and Cenozoic stratigraphy, eastern Scotian Shelf: new interpretations, Canadian Journal of Earth Sciences, v. 32, p. 1462-1473

Waldron, J.W.F., Roselli, C.G., Utting, J., and Johnston, S.K., (2010) Kennetcook thrust system: Late Paleozoic transpression near the southern margin of the Maritimes Basin, Nova Scotia, Canadian Journal of Earth Sciences, v. 47, p. 137-159
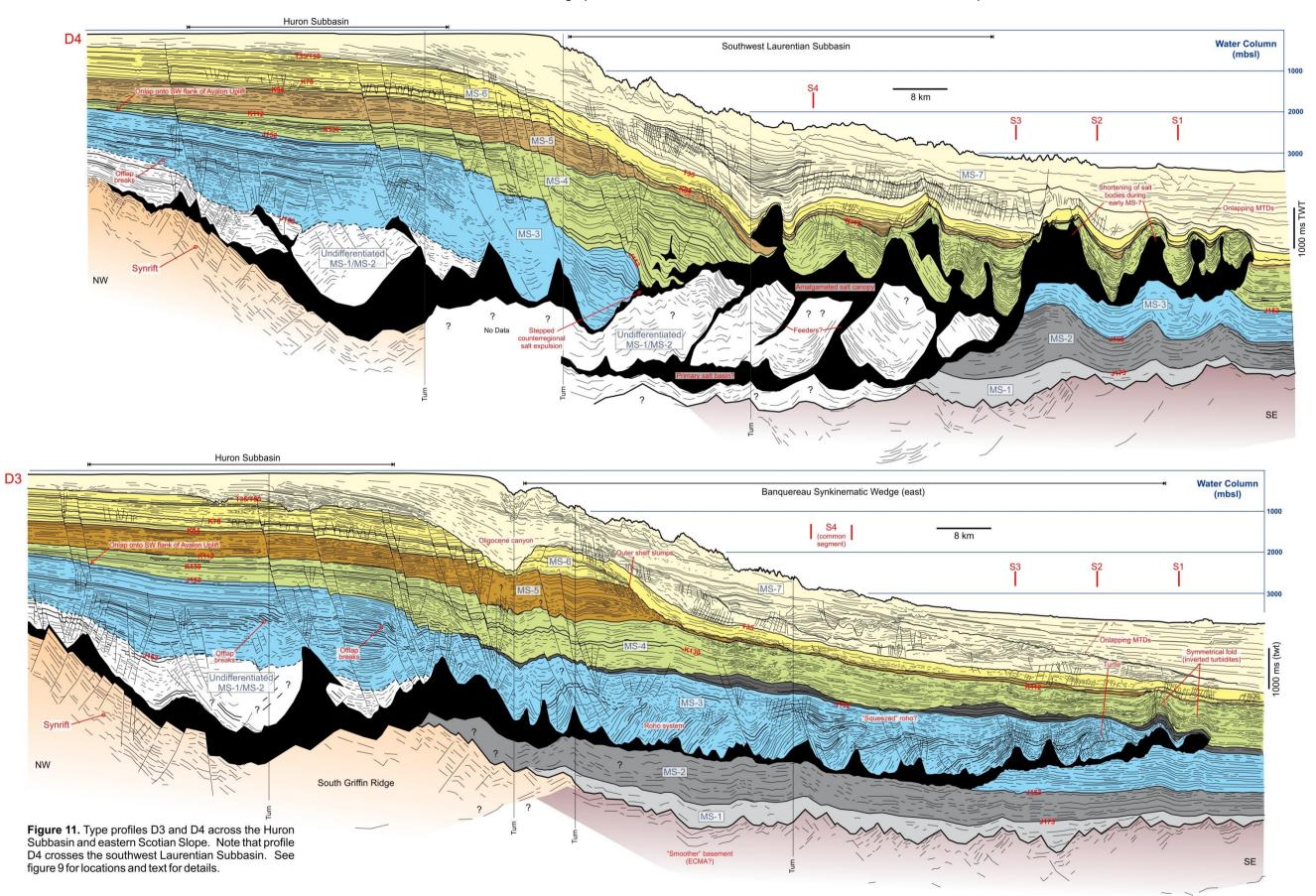
Welsink., H.J., Dwyer, J.D. and Knight, R.J. (1989) Tectono-stratigraphy of the passive margin off Nova Scotia, Chapter 14, In A.J. Tankard and H.R. Balkwill, (Eds) Extensional Tectonics and Stratigraphy of the North Atlantic Margins, AAPG Memoir 46, p. 215-231.

Weston, J.F., MacRae, R.A., Ascoli, P., Cooper, M.K.E., Fensome, R.A., Shaw, D. and Williams, G.L. (2012) A revised biostratigraphic and well-log sequence stratigraphic framework for the Scotian Margin, offshore eastern Canada, Canadian Journal of Earth Sciences, v. 49, p. 1417-1462

Wu, Y., Louden, K.E., Funck, T., Jackson, H.R. and Dehler, S.A. (2006) Crustal structure of the central Nova Scotia margin off Eastern Canada, Geophysical Journal International, no. 166, p. 878-906

Deptuck et al., 2014

Figure 10. Type profiles D1 and D2 across the Huron Subbasin and eastern Scotian Slope. See figure 9 for locations and text for details.

Figure 11. Type profiles D3 and D4 across the Huron Subbasin and eastern Scotian Slope. Note that profile D4 crosses the southwest Laurentian Subbasin. See figure 9 for locations and text for details.
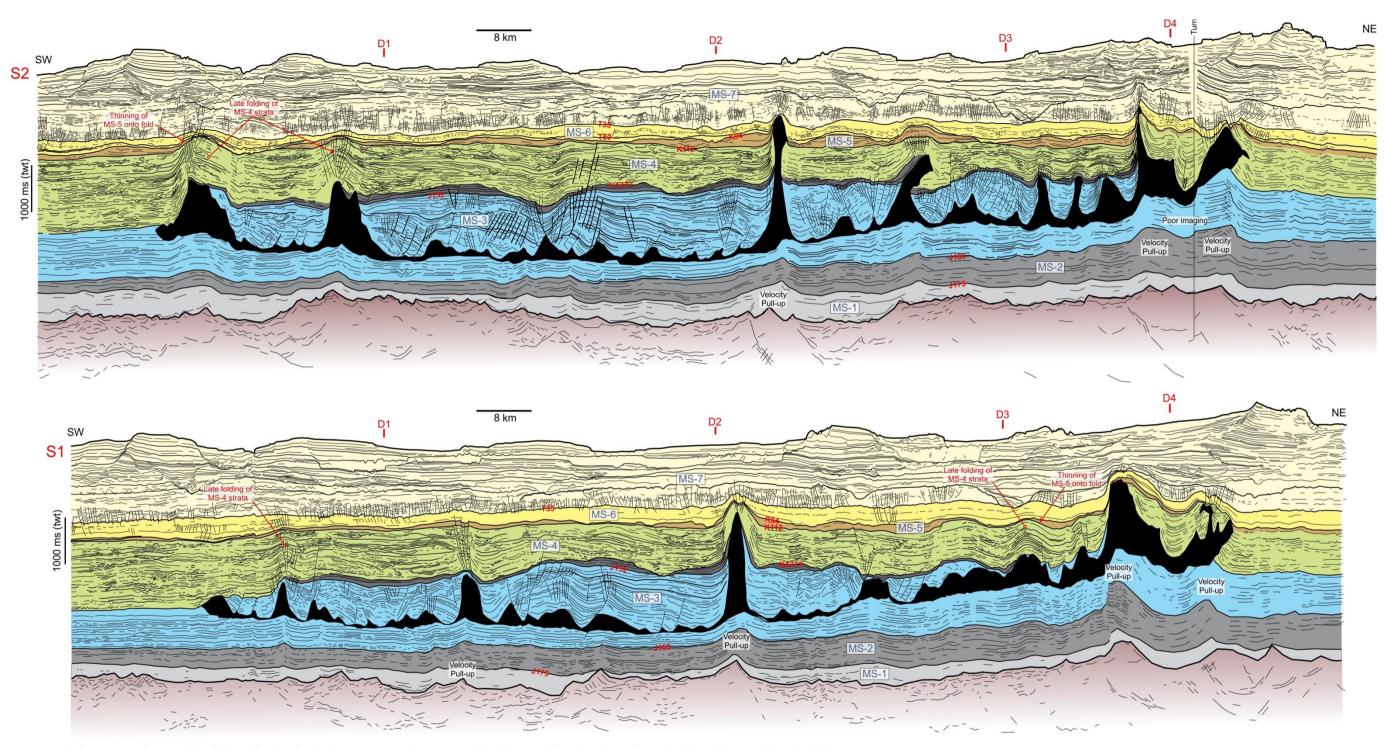
Figure 12a. Type profiles (strike-lines) S1 and S2 across the Banquereau Synkinematic Wedge.   See figure 9 for locations and text for details.

Figure 12b. Type profiles S3 and S4. Profile S4 crosses the Banquereau Synkinematic Wedge (southwest) and passes through the Southwest Laurentian Subbasin (northeast). See figure 9 for locations and text for details.